Eur. Phys. J. C 24, 495–514 (2002)
Digital Object Identifier (DOI) 10.1007/s100520200939

THE EUROPEAN PHYSICAL JOURNAL C

Quantum aspects of GMS solutions of non-commutative field theory and large N limit of matrix models*

G. Mandal[1,a], S.-J. Rey[2,b], S.R. Wadia[1,c]

[1] Department of Theoretical Physics, Tata Institute of Fundamental Research, Homi Bhabha Road, Mumbai 400 005, India
[2] School of Physics and Center for Theoretical Physics, Seoul National University, Seoul 151-747, Korea

Received: 2 January 2002 /
Published online: 26 April 2002 –

Abstract. We investigate quantum aspects of Gopakumar–Minwalla–Strominger (GMS) solutions of non-commutative field theory (NCFT) in the large non-commutativity limit, $\theta \to \infty$. Building upon a quantitative map between the operator formulation of 2- (respectively, $(2+1)$-) dimensional NCFTs and large-N matrix models of $c = 0$ (respectively, $c = 1$) non-critical strings, we show that GMS solutions are quantum mechanically sensible only if we make an appropriate joint scaling of θ and N. For 't Hooft's scaling, GMS solutions are replaced by large-N saddle-point solutions. GMS solutions are recovered from saddle-point solutions in the small 't Hooft coupling regime, but are destabilized in the large 't Hooft coupling regime by quantum effects. We make comparisons between these large-N effects and the recently studied infrared effects in NCFTs. We estimate the $U(N)$ symmetry breaking effects of the gradient term and argue that they are suppressed only in the small 't Hooft coupling regime.

1 Introduction

Non-commutative field theories (NCFT), characterized by a non-commutativity scale θ have been the subject of active research recently, largely because of the appearance of them in certain limits of the string theories and M-theory [1,2]. These NCFTs deserve further study in their own right as they exhibit many properties which are elusive, if present at all, in their commutative counterparts – such as the phenomenon of UV–IR mixing, T-duality and exact soliton/instanton (both BPS and non-BPS) solutions. One thus expects that a thorough understanding of NCFTs will shed new light on both quantum field theories and string theories.

A step toward the understanding was provided by the rich variety of classical solutions. In the large non-commutativity limit, $\theta \to \infty$, NCFT soliton/instanton solutions were constructed first by Gopakumar, Minwalla and Strominger (GMS) [3]. Exact soliton/instanton solutions were later constructed [4] for finite non-commutativity, $\theta < \infty$, as well. The classical solutions have been studied in a moduli space approximation [5,6], generalized to gauge theories [7–10], and applied to string theories in the context of tachyon condensation [11–14].

The emphasis of all these works was on finding the *classical* solutions, viz. the extrema of the NCFT action. In this paper, we would like to address *quantum mechanical* solutions and their *semiclassical limit*; equivalently, extrema of the functional integral (not just the action) of the NCFT. The first step to this goal would be to take into account the effect of the functional integral measure and study *saddle points*. We then encounter a *puzzle* immediately.

The simplest way to state this puzzle is as follows. Consider a NCFT in Euclidean two dimensions, consisting of a scalar field $\mathrm{T}(x, y)$. In operator formulation, as defined by the Weyl–Moyal map, the field $\mathrm{T}(x, y)$ is represented by $\boldsymbol{T}$, an $(\infty \times \infty)$ matrix; equivalently, an operator in an auxiliary one-particle Hilbert space $\mathcal{H}$. The formal similarity of the functional integral over $\boldsymbol{T}$ to the matrix integral of a Hermitian $(N \times N)$ matrix [15] is obvious.

An important point to note is that, in the one-matrix model, the measure of matrix integration, the famous "Coulomb repulsion" term, changes the classical vacuum dramatically [16]. Indeed, the measure effect, which scales as $\mathcal{O}(N^2)$, dominates over the classical action, which scales naively as $\mathcal{O}(N)$ *unless* a suitable scaling of the coupling parameters in the classical action is made. As we will show in Sect. 2, in the two-dimensional Euclidean NCFTs, the only way the classical action can compete with the measure effect is to take a large-θ limit in an appropriate way. Specifically, in the large-θ limit, the quantum effective action is given schematically by

$$S_{\mathrm{eff}}[\theta, N] = S_{\mathrm{classical}}[\theta, N] + S_{\mathrm{measure}}[N], \qquad (1.1)$$

* Work supported in part by BK-21 Initiative in Physics (SNU - Project 2), KRF International Collaboration Grant, KOSEF Interdisciplinary Research Grant 98-07-02-07-01-5, and KOSEF Leading Scientist Program

[a] e-mail: mandal@theory.tifr.res.in
[b] e-mail: sjrey@gravity.snu.ac.kr
[c] e-mail: wadia@theory.tifr.res.in

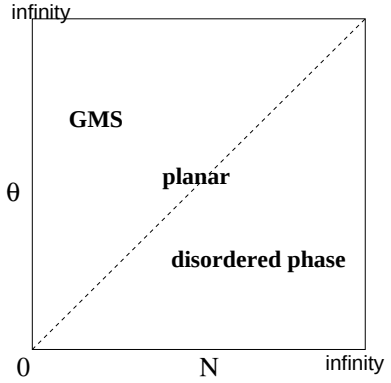

Fig. 1. Phases of two-dimensional non-commutative field theories. For $\theta \sim N^\nu$, the GMS, planar, and disordered phases correspond to $\nu > 1, = 1, < 1$, respectively

where

$$S_{\text{classical}}[\theta, N] \sim \mathcal{O}(\theta N) \quad \text{and} \quad S_{\text{measure}} \sim \mathcal{O}(N^2).$$

Clearly, there are different ways of taking a large-θ, large-N limit, leading to three distinct phases:

$$\begin{aligned} &\text{(a)} \quad \text{GMS phase}: \quad \theta \sim N^\nu \to \infty \quad (\nu > 1) \\ &\text{(b)} \quad \text{planar phase}: \quad \theta \sim N \to \infty \qquad g^2_{\text{eff}} = \text{fixed} \\ &\text{(c)} \quad \text{disordered phase}: \quad \theta \sim N^\nu \to \infty \quad (\nu < 1). \end{aligned} \tag{1.2}$$

Evidently, it is only with the scalings (a) and (b) that the classical action can compete with the term coming from the measure effect. In the limit (a) the classical term dominates, therefore the GMS solutions remains a good quantum solution. Case (b) turns out to be equivalent to the 't Hooft planar limit (see Sect. 2); in this case the measure term and the classical action are comparable, implying that the *saddle-point solutions are different from the GMS solutions*. In case (c), or for a fixed θ as is assumed for *classical* NCFT instantons, the measure effect S_{measure} becomes infinitely larger than the classical action $S_{\text{classical}}$ and indeed seems to drive the system to a different phase, referred to as the disordered phase, altogether.

The aforementioned three phases exist also for *quantum* vacua and solitons in $(2 + 1)$-dimensional NCFTs, although the way the functional integral measure effects come about is somewhat different. Evaluating the energy for vacua and solitons, we argue that quantum corrections are small for the GMS phase, but become sizable for planar and disordered phases. In particular, in the disordered phase, we find an indication that the classical vacua and solitons are destabilized completely once the measure effects are taken into account.

This paper is organized as follows. In Sect. 2, we analyze the above results for a two-dimensional Euclidean NCFT as an appropriate limit of the Hermitian one-matrix model [15] studied previously in the context of $c < 1$ non-critical strings [17]. In Sect. 3, we provide both perturbative and non-perturbative estimates of the gradient effect, which were dropped in the analysis of Sect. 2. In Sect. 4, we extend the considerations to a $(2 + 1)$-dimensional NCFT by studying its matrix model analog, viz. the time-dependent Hermitian matrix model studied previously in the context of the $c = 1$ non-critical string [18]. Among the interesting consequences caused by quantum fluctuations, we point out the spontaneous breakdown of translation invariance, and a decrease of the soliton mass. In the last section, we briefly make some remarks concerning the possible relevance of the results to IKKT [19] and BFSS [20] matrix models, and to the phenomenon of UV–IR mixing [21].

A preliminary version of this work was presented in [22].

2 Two-dimensional non-commutative field theories

2.1 Classical theory

Let us begin with the non-commutative plane $\mathbb{R}^2_\theta$, whose coordinates $\boldsymbol{y}$ obey the Heisenberg algebra:

$$[y^a, y^b] = \mathrm{i}\theta^{ab} = \mathrm{i}\theta\epsilon^{ab} \quad (a, b = 1, 2). \tag{2.1}$$

We shall be studying a Euclidean field theory on $\mathbb{R}^2_\theta$, consisting of a scalar field $\mathrm{T}(\boldsymbol{y})$ with self-interaction potential – in general polynomial – $V(\mathrm{T})$. Via the Seiberg–Witten map [2], the theory can be described equivalently in terms of a non-commutative field theory (NCFT) on $\mathbb{R}^2$, whose action is given by

$$S_{\text{NC}}[\theta; V] = \int_{\mathbb{R}^2} \mathrm{d}^2\boldsymbol{y} \left[\frac{1}{2}\partial_{\boldsymbol{y}}\mathrm{T} \star_\theta \partial_{\boldsymbol{y}}\mathrm{T} + V_{\star_\theta}(\mathrm{T})\right]. \tag{2.2}$$

In NCFT, the non-commutativity θ^{ab} is encoded through the $\star_\theta$-product

$$\begin{aligned} (A \star_\theta B)(\boldsymbol{y}) := \exp\left(\frac{\mathrm{i}}{2}\theta^{ab}\partial^a_{\boldsymbol{y}_1} \wedge \partial^b_{\boldsymbol{y}_2}\right) \\ \times A(\boldsymbol{y}_1)B(\boldsymbol{y}_2)|_{\boldsymbol{y}_2=\boldsymbol{y}_1=\boldsymbol{y}}. \end{aligned} \tag{2.3}$$

It has been noted that a theory of the type (2.2) arises for the level-zero truncation of the open string field theory on a Euclidean worldvolume of an unstable D1-brane, either in bosonic or in Type IIA string theories, on which a non-zero, constant background of the (Euclideanized) two-form potential B_2 is turned on [23]. The scalar field $\mathrm{T}(\boldsymbol{x})$ in (2.2) represents, when expanded around the top of the potential $V(\mathrm{T})$, a real-valued tachyon field in these situations.

The inverse of the non-commutativity parameter, $1/\theta$, plays the role of a coupling parameter of the NCFT. To see this, rescale the coordinates as

$$\boldsymbol{y} \quad \to \quad \boldsymbol{x} = \frac{1}{\sqrt{\theta}}\boldsymbol{y} \quad \text{so} \quad \text{that} \quad \left[x^a, x^b\right] = \mathrm{i}\epsilon^{ab}$$

and expand the NCFT action (2.2) in powers of $(1/\theta)$:

$$S_{\text{NC}}[\theta; V_\star] = \theta \int_{\mathbb{R}^2} \mathrm{d}^2\boldsymbol{x} \left[\mathcal{L}_0 + \frac{1}{\theta}\mathcal{L}_{-1} + \cdots\right]. \tag{2.4}$$

Here,

$$\mathcal{L}_0 = V_\star(\mathrm{T}) \quad \text{and} \quad \mathcal{L}_{-1} = \frac{1}{2}\left(\partial_{\boldsymbol{x}}\mathrm{T}\right)^2, \tag{2.5}$$

and the $\star$'s refer to the Moyal product (2.3) in which the non-commutativity parameter θ^{ab} is replaced by ϵ^{ab}. Evidently, for large non-commutativity, $(1/\theta) \to 0$, the gradient term $\mathcal{L}_{-1}$ yields a sub-leading order correction[1].

Utilizing the Weyl–Moyal map (See Appendix A), one can map the two-dimensional NCFT (2.2) to a *zero*-dimensional Hermitian matrix model, defined by

$$\mathbb{S}_{\mathrm{NC}}[\theta; V] = \theta \mathrm{Tr}_{\mathcal{H}} \left[V(\boldsymbol{T}) + \frac{1}{\theta}\left(-\frac{1}{2}\left[\hat{\boldsymbol{x}}, \boldsymbol{T}\right]^2\right) + \cdots \right]. \tag{2.6}$$

2.2 Classical vacua and instantons

Classical solutions of the NCFT are most straightforwardly obtainable from (2.6). At leading order in $\theta \to \infty$, the classical solutions are critical points of the potential, $V'(\boldsymbol{T}) = 0$, viz. a matrix-valued algebraic equation of degree $(P-1)$. Let us denote the local minima of the polynomial function $V(\lambda)$ as $\lambda_0, \lambda_1, \lambda_2, \cdots$, conveniently labelled in ascending order: $V(\lambda_0) \le V(\lambda_1) \le V(\lambda_2) \le \cdots$.

One then finds that the most general classical solution of $V'(\boldsymbol{T}) = 0$ takes the form

$$\boldsymbol{T} = \sum_{\ell=1}^{N} \lambda_{a_\ell} \boldsymbol{P}_\ell,$$

where the λ_{a_ℓ}'s take values out of the set $(\lambda_0, \lambda_1, \cdots)$ permitting duplications. We will define the eigenvalue density $\rho(\lambda)$ by

$$\rho(\lambda) := \frac{1}{\dim\mathcal{H}} \sum_a \delta(\lambda - \lambda_a). \tag{2.7}$$

As a concrete example, consider a symmetric double-well potential:

$$V(\boldsymbol{T}) = V_0 + \frac{\lambda_4}{4}\left(\boldsymbol{T}^2 - \mathrm{T}_0^2\right)^2, \tag{2.8}$$

for which the roots λ_a are $\pm\mathrm{T}_0$.

Vacua

Using (2.7), we easily find the doubly degenerate vacua (R and L, for left and right), given by

$$\boldsymbol{T}_{\mathrm{R,L}} = \pm\mathrm{T}_0 \mathbb{I}. \tag{2.9}$$

These solutions are exact and are valid for any θ, small or large. The energy E_0 is given by $E_0 = (N\theta)V_0$.

[1] Quantum mechanically, somewhat surprisingly, the $\mathcal{L}_{-1}$ term contributes leading order effects in the planar expansion in powers of $1/N$. In Sect. 3, we will show that a small 't Hooft coupling suppresses the contribution compared to those from the $\mathcal{L}_0$ term

Instantons

The other solutions, using (2.7), are given by

$$\boldsymbol{T}_{N_1,N_2} = \mathrm{T}_0\left(\boldsymbol{P}_{[N_1]} - \boldsymbol{P}_{[N_2]}\right). \tag{2.10}$$

These solutions are generally valid only for large θ, with $\mathcal{O}(1/\theta)$ corrections affecting both their profile and their energy. The notation $\boldsymbol{P}_{[N_1]}$ stands for a projection operator of rank N_1, and similarly for N_2. We will call the solution (2.10) an "(N_1, N_2) instanton".

From (2.7), we find that the above vacua and instantons yield the following density profiles:

$$\rho_{\mathrm{R,\,L}}(\lambda) = \delta(\lambda \mp \mathrm{T}_0),$$
$$\rho_{[N_1,N_2]}(\lambda) = n_1\delta(\lambda - \mathrm{T}_0) + n_2\delta(\lambda + \mathrm{T}_0),$$

where

$$n_{1,2} = \frac{N_{1,2}}{\dim\mathcal{H}}. \tag{2.11}$$

2.3 Quantum theory

Definition

The quantum NCFT is defined via the following *regularized* partition function:

$$\mathcal{Z}_{\mathrm{NC}}[\theta, V_\star; L_1 L_2] = \int [\mathrm{dT}]_{L_1,L_2} \exp(-S_{\mathrm{NC}}[\theta; V_\star]), \tag{2.12}$$

where S_{NC} is given by (2.4). Here L_1, L_2 represent large distance cutoffs introduced as regulator of possible infrared divergences. Generically, the theory also needs an ultraviolet cutoff, e.g. a lattice spacing a; the theories discussed in this paper will be taken to be ultraviolet-renormalizable. We will assume that in the above definition (2.12) the limit $a \to 0$ has been taken.

In the previous section, we have seen that a classical NCFT is equivalent, via the Weyl–Moyal correspondence, to a model of a $(\infty \times \infty)$ Hermitian matrix, (2.6). What then would be the corresponding statement at the quantum level? As the theory (2.12) is *defined* with the large distance cutoffs L_1, L_2, one is naturally led to a non-commutative torus (see, e.g. [1]) as a concrete setup for infrared regularization; see Fig. 2 for an illustration.

Let us start with a non-commutative torus $\mathbb{T}^2_\theta$, defined through the so-called quotient condition on the $(N \times N)$ matrices X^1, X^2 by

$$X^a + L^a\delta^a_b \mathbb{I}_N = \mathsf{U}_b^{-1} X^a \mathsf{U}_b \quad (a, b = 1, 2).$$

Generically, a non-trivial solution to the quotient condition requires $N \to \infty$. Applying the condition in two different directions on $\mathbb{T}^2_\theta$, one finds that the quotients U_a ought to obey

$$\mathsf{U}_a\mathsf{U}_b\mathsf{U}_a^{-1}\mathsf{U}_b^{-1} = \mathrm{e}^{-\mathrm{i}\Theta^{ab}}\mathbb{I},$$

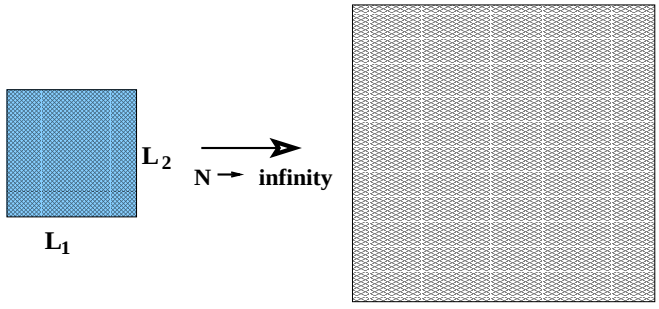

Fig. 2. Non-commutative plane as a continuum and large-volume limit of the non-commutative torus. The limit requires $N \to \infty$

where Θ_{ab} is dimensionless and will shortly be identified, for a square torus, with $\Theta^{ab} = \theta^{ab}(2\pi/L)^2$ ($L_1 = L_2 = L$).

The scalar field $\boldsymbol{T}$ defined on $\mathbb{TT}^2_\theta$ is defined via

$$\boldsymbol{T} = \sum_{\{\boldsymbol{m}\}=\mathbb{Z}} \widetilde{\boldsymbol{T}}_{\boldsymbol{m}} \mathsf{U}_1^{m_1} \mathsf{U}_2^{m_2}.$$

Here, $\widetilde{\boldsymbol{T}}_{\boldsymbol{m}}$ belongs to a sufficiently rapidly decreasing sequence of the appropriate Schwartz space.

One can represent the $\mathsf{U}_1, \mathsf{U}_2$ basis in terms of Hermitian operators of the form

$$\mathsf{U}_a = \exp\left(2\pi \mathrm{i} \frac{\boldsymbol{y}^a}{L^a}\right) \quad (a = 1, 2),$$

where, in the large-N limit,

$$\left[\widehat{y^a}, \widehat{y^b}\right] \approx \mathrm{i}\left(\frac{L_a L_b}{(2\pi)^2}\right) \Theta^{ab} \equiv \mathrm{i}\ \theta^{ab},$$

in which we have used (2.1) in the last step.

The simplest situation arises for so-called rational non-commutative tori. For our purposes it is sufficiently general to consider, among these, the case when

$$\Theta^{ab} = \Theta \epsilon^{ab} \quad \text{and} \quad \Theta = n/N \quad (n = 1, 2, \cdots, N). \tag{2.13}$$

Focusing on the square torus $L_1 = L_2 = L$ from now on, we get, using the above two equations,

$$\theta = \left(\frac{L}{2\pi}\right)^2 \Theta = \left(\frac{L}{2\pi}\right)^2 \frac{n}{N}. \tag{2.14}$$

For the non-commutative torus with such a value of θ, the Weyl–Moyal correspondence maps the partition function (2.12) of the NCFT on $\mathbb{TT}^2_\theta$ to the following partition function for a Hermitian matrix of size $(N \times N)$:

$$\mathsf{Z}_N[\Theta, V; N] = \int [\mathrm{d}\boldsymbol{T}]_N \exp(-\$_{\mathrm{NC}}[\Theta; V(\boldsymbol{T})]), \tag{2.15}$$

where the matrix integral measure is given by

$$[\mathrm{d}\boldsymbol{T}]_N := \prod_{i=1}^{N} \mathrm{d}\boldsymbol{T}_{ii} \prod_{1 \le i < j \le N} 2\mathrm{dRe}(\boldsymbol{T}_{ij}) \mathrm{dIm}(\boldsymbol{T}_{ij}).$$

Let us now consider the limit $L \to \infty$; in this limit the non-commutative torus $\mathbb{TT}^2_\theta$ ought to approach the non-commutative plane $\mathbb{R}^2_\theta$. Since the Heisenberg algebra (2.1) on $\mathbb{R}^2_\theta$ has only infinite-dimensional representations, the above limit must also be accompanied by a limit $N \to \infty$. As $\theta \sim L^2(n/N)$ from (2.14), the large-θ limit discussed in Sect. 2.1 can be attained by

$$L \to \infty, \quad N \to \infty, \quad n \to \infty \quad \text{and} \quad \theta \sim L^2(n/N) \to \infty.$$

This is achievable by letting

$$L \sim N^\gamma, \quad n \sim N^\alpha \quad \Rightarrow \quad \theta \sim N^\nu,$$

where

$$\nu = (2\gamma - (1 - \alpha)), \tag{2.16}$$

and we take[2]

$$\alpha < 1 \quad \text{and} \quad \gamma > \frac{1}{2}(1 - \alpha) \to \nu > 0.$$

To sum up, the above observations lead to the definition of the quantum NCFT on $\mathbb{R}^2_\theta$ as follows:

$$\lim_{L_1 L_2 \to \infty} \mathcal{Z}_{\mathrm{NC}}[\theta, V_\star; L_1 L_2] \equiv \lim_{N \to \infty} \mathsf{Z}_N[\theta, V; N], \tag{2.17}$$

where, on the right-hand side, the non-commutativity parameter θ is given in terms of (2.14).

2.4 Classical, planar, and disordered phases of NCFT$_2$

The Weyl–Moyal equivalence (2.17), together with (2.16), indicates that the quantum NCFT is actually defined in terms of a double-series expansion: large-N, and large-θ expansions. To give details, let us define the quantum NCFT in terms of the Hermitian matrix model, as in the right-hand side of (2.17). Suppose, at large θ, we ignore the subleading part $\mathcal{L}_{-1}$ in the action (2.4). In that case, the partition function becomes identical in form to the one-matrix integral [15] and the $c < 1$ matrix models for $c < 1$ non-critical strings [17]. These latter models are defined in terms of the matrix model partition function $\mathbb{Z}_{\mathrm{mm}}$

$$\mathbb{Z}_{\mathrm{mm}}[\beta, V; N] = \int \mathrm{d}\boldsymbol{M} \exp(-\beta \mathrm{Tr}_N V(\boldsymbol{M})), \tag{2.18}$$

where $V(x)$ is the Boltzmann function, taking a polynomial form: $V(x) = a_2 x^2 + a_4 x^4 + \ldots$. Evidently, modulo the identification $\theta = \beta$, we have

$$\mathsf{Z}_N[\theta, V; N] \quad = \quad \mathbb{Z}_{\mathrm{mm}}[\beta, V; N]. \tag{2.19}$$

[2] In the regularization adopted, the ultraviolet cutoff in the momenta $p_a \equiv \mathrm{i}\partial_{y_a}$ turns out to be $\Lambda_{\mathrm{uv}} = N/L$, as the highest Fourier modes are set by $\sim \mathsf{U}_1^N, \mathsf{U}_2^N$. Our scalings should ensure $\Lambda_{\mathrm{uv}} \to \infty$. This is readily achievable by imposing the additional condition $\gamma < 1$

To investigate the partition function Z_N, we will therefore proceed as in the case of the one-matrix model. Integrating out the "angular part" of $\boldsymbol{T}$, the partition function Z_N is rewritable as an integral over the N eigenvalues $\lambda_1, \lambda_2, \cdots, \lambda_N$ of $\boldsymbol{T}$ [15]:

$$\begin{aligned}\mathsf{Z}_N[\theta, V; N] &= C_N \int \prod_{k=1}^{N} \mathrm{d}\lambda_k \prod_{k<\ell}^{N} (\lambda_k - \lambda_\ell)^2 \\ &\quad \times \exp\left(-\theta \sum_k V(\lambda_k)\right) \qquad (2.20) \\ &= C_N \int \prod_{k=1}^{N} \mathrm{d}\lambda_k \exp(-S_{\mathrm{eff}}(\lambda_1, \cdots, \lambda_N)),\end{aligned}$$

where

$$C_N = \mathrm{Vol}\left[\frac{\mathrm{U}(N)}{\mathrm{U}(1)^N \times \mathcal{S}_N}\right] = \frac{1}{N!} \prod_{K=1}^{N} \frac{(2\pi)^{K-1}}{\Gamma(K)}$$

refers to the angular volume measure factor, and

$$S_{\mathrm{eff}}(\lambda_1, \cdots, \lambda_N) = S_{\mathrm{classical}}[N, \theta] + S_{\mathrm{measure}}[N], \quad (2.21)$$

with

$$S_{\mathrm{classical}}[N, \theta] = N\theta \left(\frac{1}{N} \sum_{k=1}^{N} V(\lambda_k)\right)$$

and

$$S_{\mathrm{measure}}[N] = N^2 \left(\frac{1}{2N^2} \sum_{1 \le k \ne \ell \le N} \ln(\lambda_k - \lambda_\ell)^2\right)$$

referring to the effective action as a sum of the classical contribution and the measure factor contribution.

The large-N limits of one-matrix models are describable by a *master field* configuration, where the distribution of the eigenvalues $\lambda_1, \cdots, \lambda_N$ is encoded in the density field $\rho(\lambda)$, introduced in (2.7), with support over connected compact domains $\mathcal{D}$ and subject to the constraints

$$\int_{\mathcal{D}} \mathrm{d}\lambda \rho(\lambda) = 1 \qquad \text{and} \quad \rho(\lambda) \ge 0 \quad \text{on} \quad \lambda \subset \mathcal{D}. \quad (2.22)$$

The effective action of the eigenvalues then becomes

$$\begin{aligned}S_{\mathrm{eff}}[\rho] = N^2 \Bigg[& g_{\mathrm{eff}}^{-2} \int_{\mathcal{D}} \mathrm{d}\lambda \rho(\lambda) V(\lambda) \\ & - \int_{\mathcal{D}} \mathrm{d}\lambda \int_{\mathcal{D}} \mathrm{d}\mu \rho(\lambda) (\ln|\lambda - \mu|) \rho(\mu) \Bigg], \qquad (2.23)\end{aligned}$$

in which

$$g_{\mathrm{eff}}^2 \equiv \frac{N}{\theta} \qquad (2.24)$$

measures the relative weight between the classical contribution and the measure factor contribution.

Now the effective action (2.23) is exactly of the form (1.1). One thus discovers that, in *quantum* NCFT, there ought to exist three distinct regimes as in (1.2). If one were to define the quantum NCFT in terms of the Hermitian matrix model, as in (2.17), via the Weyl–Moyal equivalence, the three different regimes are distinguished by relative weights in (2.23) of the classical contribution $S_{\mathrm{classical}} \sim \mathcal{O}(N\theta)$ and the matrix integral measure part contribution $S_{\mathrm{measure}} \sim \mathcal{O}(N^2)$.

The above considerations entail an important consequence for the interpretation of the non-commutative field theories and the classical solutions therein, as studied in [3]. First, in non-commutative field theory, one defines the theory by viewing the non-commutative field T as a representation of the Heisenberg algebra, which is infinite-dimensional in case the theory is defined on $\mathbb{R}^2_\theta$. If one interprets this as meaning that the size N of the matrix field $\boldsymbol{T}$ is strictly infinite to begin with, then the classical action $S_{\mathrm{classical}}$ becomes insignificant, as it is far outweighed by the quantum contribution S_{measure} coming from the matrix-integral measure. Second, in order to be able to view the classical solutions, e.g. solutions studied in [3], as saddle points of the partition function (2.12), one must first "regulate" the non-commutative field theory in such a way that the corresponding Weyl formulation is defined on a finite N-dimensional Hilbert space to begin with, viz. the Hermitian matrix model is for $(N \times N)$ matrices. In order to recover a sensible saddle-point solution, one *subsequently* needs to take an appropriate large-θ, large-N limit. Equation (1.2) indicates that, a priori, there are three types of possible scaling of the non-commutative field theory. Based on this observation, we thus conclude that, only in the classical scaling (a) the classical solutions found in [3] are also the saddle-point solutions. For the planar scaling (b), the classical solutions ought to be replaced, as we will find in the next section, by new ones in which the eigenvalues are distributed. In the disordered scaling (c) of (1.2), the classical solutions found in [3] are washed out completely.

2.5 Quantum vacua and instantons

We now flesh up the preceding discussion by studying the *quantum* vacua and instantons of the two-dimensional NCFT on $\mathbb{R}^2_\theta$ in the large-N, large-θ limit in the various regimes (1.2). In doing so, we will use the analogy (2.19) with the one-matrix model studied in the context of the $c < 1$ non-critical string [17] to quantize the solutions described in Sect. 2.2. We will do explicit calculations in the GMS and planar phases and will make some qualitative remarks about the disordered phase.

We begin by defining the "free" energy $F[\theta, V; N]$ by

$$\mathsf{Z}_N[\theta, V; N] := \left(\frac{2\pi}{N}\right)^{N^2/2} \mathrm{e}^{-F[\theta, V; N]},$$

where the normalization is chosen so that $F = 0$ for the quadratic potential $V(\boldsymbol{T}) = (1/2)\mathrm{Tr}\boldsymbol{T}^2$. As is well known [15], the free energy has the following large-N expansion:

$$F[\theta = (N/g_{\rm eff}^2), N] = N^2 F_0(g_{\rm eff}^2) + F_1(g_{\rm eff}^2) + N^{-2} F_2(g_{\rm eff}^2) + \ldots, \quad (2.25)$$

where each of the F_n is defined via a power series in $g_{\rm eff}^2$ with a radius of convergence $g_{\rm c}$. It will be convenient in this stage to rephrase the three limits (1.2):

(a) GMS phase : $N \to \infty, \quad g_{\rm eff} \to 0$
(b) planar phase : $N \to \infty, \quad g_{\rm eff} = \text{fixed}$
(c) disordered phase : $N \to \infty, \quad g_{\rm eff} \to \infty.$ (2.26)

The leading term F_0 in (2.25) is given by the saddle-point contribution in the large-N limit. Clearly, the leading behavior of (a) the GMS-phase free energy, and (b) the planar-phase free energy (for $g_{\rm eff} < g_{\rm c}$) are derivable from this saddle-point expression. The disordered-phase free energy is clearly in the strong coupling phase $g_{\rm eff} > g_{\rm c}$ in which the large-N expansion (2.25) breaks down.

We see, therefore, that we can derive the leading behavior of the partition function Z_N in the double limit, $N \to \infty, \theta \to \infty$, from the large-$N$ saddle point (except in the disordered phase). We describe in Appendix B how to compute the large-N saddle points as minima of the effective action (2.23) subject to the constraint (2.22). We simply quote the result here (see Appendix B or [15,24] for more details of the derivation).

For the double-well potential of the type (2.8), the saddle-point density is given in terms of two-cut eigenvalue distribution[3]:

$$\rho_{\rm s}(\lambda) = \begin{cases} \frac{1}{2} g_{\rm eff}^{-2} \sqrt{\lambda^2(\lambda^2 - \lambda_-^2)(\lambda_+^2 - \lambda^2)} \\ \quad \text{for} \quad \lambda \in (-\lambda_+, -\lambda_-) \cup (\lambda_-, \lambda_+), \\ 0 \quad \text{otherwise.} \end{cases} \quad (2.27)$$

Here

$$\lambda_- = \sqrt{(\mathrm{T}_0 - 2g_{\rm eff}^2)}, \quad \lambda_+ = \sqrt{(\mathrm{T}_0 + 2g_{\rm eff}^2)}.$$

As explained above, (2.27) is the leading large-N, large-θ value of the quantum corrected density function, in the planar limit (b), corresponding to the classical (N_1, N_2) instanton of Sect. 2.2 for $N_1 = N_2$.

Equation (2.27) is clearly different from the classical (GMS) value ((2.11) with $N_1 = N_2$). But from what we have discussed above, we expect to recover the classical (GMS) value in the weak 't Hooft coupling limit, $g_{\rm eff} \to 0$. This is indeed what happens. In this limit, the eigenvalue density, (2.27), reduces to

$$\rho_{\rm s}(\lambda) \longrightarrow \rho_{\rm classical}(\lambda) = \frac{1}{2}\delta(\lambda - \mathrm{T}_0) + \frac{1}{2}\delta(\lambda + \mathrm{T}_0).$$

This is identical with (2.11) for

$$N_1 = N_2 = \frac{N}{2} \quad \text{equivalently} \quad n_1 = n_2 = \frac{1}{2}.$$

[3] We assume $g_{\rm eff}^2 < T_0/2$ so that the parameters $\lambda_\pm$ are real-valued. At $g_{\rm eff}^2 = T_0/2$, λ_- vanishes and the two cuts merge into one cut, signifying a spill-over of eigenvalues from each potential well into the other

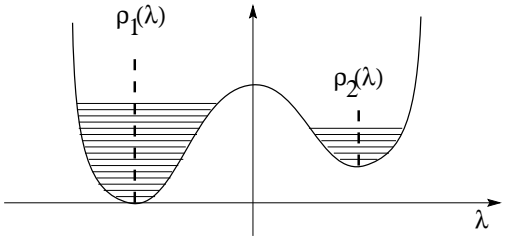

Fig. 3. Eigenvalue distributions for non-commutative vacua and instantons. Classically, the eigenvalues are piled up to a delta-function type distribution, as depicted as the dashed line. Quantum mechanically, the eigenvalues repel each other and are spread over, as depicted by the horizontal lines

It is worth mentioning that for the scaling (b) the classical limit $g_{\rm eff} \to 0$ of the planar saddle-point configuration is not necessarily the same as the classical regime (a). As the result (2.27) for the double-well potential exemplifies, the "classical limit" $g_{\rm eff} \to 0$ yields, out of N possible classical instantons of type (N_1, N_2), the one with $N_1 = N_2 = N/2$ singled out.

In fact, it is possible to visualize the quantum instantons as *non-interacting* quantum vacua, localized at λ_- and λ_+, respectively. Consider the situation that the two potential wells are widely separated and contain N_1, N_2 eigenvalues, respectively. Then the partition function reads

$$\mathsf{Z}[\theta, V; n_1, n_2] = \int_{-\infty}^{\Lambda} \prod_{k=1}^{N_1} \mathrm{d}\lambda_k \int_{\Lambda}^{+\infty} \prod_{\ell=N_1}^{N} \mathrm{d}\lambda_\ell \prod_{1 \le k < \ell \le N} (\lambda_k - \lambda_\ell)^2 \times \exp(-\$_{\rm NC}[\theta, V; N_1, N_2]).$$

Here, Λ denotes a suitably chosen, midpoint "cutoff" value of the eigenvalue between the two cuts. In fact, the above partition function is expressible as a matrix integral over two separate matrices: $\boldsymbol{T}_1$ of size $(N_1 \times N_1)$ and $\boldsymbol{T}_2$ of size $(N_2 \times N_2)$, whose eigenvalues are restricted to be less than or larger than Λ, respectively. One easily finds that

$$\mathsf{Z}[\theta, V; n_1, n_2] = \int [\mathrm{d}\boldsymbol{T}_1]_{N_1} \int [\mathrm{d}\boldsymbol{T}_2]_{N_2} \exp(-\$_{\rm NC}[\theta, V; N_1, N_2]),$$

where

$$\$_{\rm NC} = \theta \left[\mathrm{Tr} V(\boldsymbol{T}_1) + \mathrm{Tr} V(\boldsymbol{T}_2)\right] + \left[2\mathrm{Tr}\left(\ln(\boldsymbol{T}_1 \otimes \mathbb{I} - \mathbb{I} \otimes \boldsymbol{T}_2)\right) + \cdots\right], \quad (2.28)$$

in which the ellipses denote gradient corrections. The above effective two-matrix integral is well defined in the large-N, large-θ limit. Evidently, at leading order in a $(1/\theta)$ expansion, the matrix integral is factorized into two disjoint one-matrix integrals, except that the eigenvalues are bounded from above and below, respectively. The saddle-point configuration is described precisely by the above solution. The error involved in the ellipses in (2.28) is of order $\mathrm{e}^{-\mathcal{O}(N)}$, due to the tunnelling effect, and hence is completely negligible in the continuum limit.

2.6 Quantum corrections

The central observation in the foregoing discussion was that the quantum effects drive the eigenvalues to repel each other – a dramatic change when compared to the situation at the classical level. To demonstrate how striking the quantum effects are, let us compute the "quantum" Euclidean action and compare its ground-state value with that of the classical action. The second order perturbation theory asserts that, around the ground state, quantum corrections to physical quantities are typically negative. Thus, one would expect that, once the quantum corrections are taken into account, the Euclidean action gets lowered. In quantum NCFT, quite to the contrary, we will find that the quantum effects *increase* the Euclidean action! This has to do with the fact that the repulsion among the eigenvalues is a purely quantum mechanical effect, not present at the classical level at all.

Let us begin with the effective action of the eigenvalue density field, $\rho(\lambda)$, (2.23). The saddle-point configuration is governed by solutions of (B.2). We shall be taking a generic condition that the classical potential $V(\lambda)$ is a concave function of λ with a global minimum at $\lambda = \lambda_{\rm s}$ and denote $V(\lambda_{\rm s}) = V_0$. Evidently, $V(\lambda) \geq V_0$ for all λ. Multiplying (B.2) with $\rho_{\rm s}(\lambda)$ and then integrating over λ, we obtain

$$N^2 \left[g_{\rm eff}^{-2} \int_{\mathcal{D}} {\rm d}\lambda \rho_{\rm s}(\lambda) V(\lambda) - 2 \int {\rm d}\mu {\rm d}\lambda \rho_{\rm s}(\mu) \ln|\lambda - \mu| \rho_{\rm s}(\lambda) \right] = N\theta E,$$

where we have used the normalization condition, $\int {\rm d}\lambda \rho_{\rm s}(\lambda) = 1$, and E is the first integral of motion. Using this relation, the quantum Euclidean action (2.23) is re-expressible as

$$\begin{aligned} S_{\rm eff}[\rho_{\rm s}] &= N^2 \left[g_{\rm eff}^{-2} \int_{\mathcal{D}} {\rm d}\lambda \rho_{\rm s}(\lambda) V(\lambda) - \int_{\mathcal{D}} {\rm d}\lambda \int_{\mathcal{D}} {\rm d}\mu \rho_{\rm s}(\lambda) \ln|\lambda - \mu| \rho_{\rm s}(\mu) \right] \\ &= N\theta E + \frac{1}{2} N\theta \left(\int {\rm d}\lambda \rho_{\rm s}(\lambda) V(\lambda) - E \right). \end{aligned} \quad (2.29)$$

The first integral of motion E is fixed uniquely to $E = N\theta V_0$ by demanding that, in the weak 't Hooft coupling limit, $g_{\rm eff} \to 0$, and the saddle-point value of the quantum Euclidean action (2.29) reduces to that of the classical Euclidean action, $S_{\rm classical} = N\theta V_0$. Thus, one readily finds that the second term in (2.29) amounts to a change of the Euclidean action due to quantum effects.

Let us now evaluate the second term in (2.29), the quantum correction to the Euclidean action. First of all, from the expression, the problem whether the correction is negative – as the second order perturbation theory suggests – or not is easily analyzable. Classically, the N species of eigenvalues were all sitting at a single point $\lambda = \lambda_{\rm s}$, but, once the quantum effects are taken into account, they will repel each other and form a domain, denoted in (2.29) by $\mathcal{D}$, of an eigenvalue distribution around the point $\lambda = \lambda_{\rm s}$. Take a generic point λ inside $\mathcal{D}$. As $V(\lambda) \geq V_0$ by the definition of $\lambda_{\rm s}$ and $\rho_{\rm s}(\lambda)$ is distributed over $\mathcal{D}$, it follows immediately that

$$\begin{aligned} \Delta E &:= (S_{\rm eff} - N\theta E) \\ &= \frac{1}{2} N\theta \left(\int_{\mathcal{D}} {\rm d}\lambda \rho_{\rm s}(\lambda) V(\lambda) - E \right) \\ &= \frac{1}{2} N\theta \int_{\mathcal{D}} {\rm d}\lambda \rho_{\rm s}(\lambda) (V(\lambda) - V_0) \\ &\geq 0. \end{aligned} \quad (2.30)$$

This proves that the quantum correction in (2.29) is positive, in contrast to what one expects from the second order perturbation theory. Evidently, the reason has to do with eigenvalue repulsion – classically invisible but a quantum mechanically generated effect. The repulsion gives rise to a positive "pressure", resulting in an increase of the Euclidean action.

We now compute the increment of the Euclidean action explicitly. We will take, for simplicity, $V(\lambda) = (1/2)\lambda^2$ – an approximation applicable, at leading order, for each cut of a generic concave potential, according to the result of (2.28). Utilizing (B.3) (see also [15]), it is straightforward to compute $\rho_{\rm s}(\lambda)$. We find

$$\rho_{\rm s}(\lambda) = \frac{1}{2\pi} \sqrt{4 - \lambda^2} \quad \text{for} \quad -2 \leq \lambda \leq +2. \quad (2.31)$$

Substituting (2.31) into (2.30), we obtain (recall that here the classical energy is normalized as $N\theta E = 0$)

$$\begin{aligned} \Delta E = S_{\rm eff}[\rho_{\rm s}] &= N\theta \int_0^2 {\rm d}\lambda \frac{1}{2\pi} \sqrt{4 - \lambda^2} \cdot \frac{1}{2} \lambda^2 \\ &= \frac{1}{4} N\theta. \end{aligned}$$

Thus, the correction is of order N^2 in the planar phase (b) of (2.26).

We conclude this section by mentioning that quantum corrections in the disordered phase cannot be calculated by the above procedure, as the large-N saddle point is irrelevant. It is readily seen, however, that the quantum corrections in the disordered phase will be larger. In the example analyzed below, we will see that $(\Delta E)_{\rm Q} / (\Delta E)_{\rm planar} \to \infty$ in the disordered phase (c) of (1.2).

2.7 Perturbative manifestation of the Vandermonde effect

The effect of $S_{\rm measure}$ in (2.21), being originating in the Vandermonde determinant of the functional integral measure, ought to be obtainable in the standard Feynman diagrammatics. How do the effects manifest themselves? We will now show that, in the context of the Feynman diagrammatics in Weyl formulation, the aforementioned limits (1.2) or (2.26) are derivable in the large-θ and large-L limit[4].

[4] Related remarks are also made in [25], though some of the interpretations are in contrast to ours

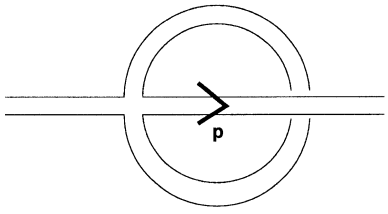

Fig. 4. One-loop, non-planar contribution to the two-point Green function

We begin with the Feynman rules defined in the Moyal formulation by (2.12) and the potential (2.8). Our objective is to see how the quantum corrections differ in the three scaling regimes, (1.2). In computing the effects, we keep in mind the relations (2.14) between the parameters (L,θ) of $\mathbb{TT}^2_\theta$ and the parameters (N,θ) of $\mathbb{R}^2_\theta$.

Expand the action around the "right vacuum" $\mathrm{T}(\boldsymbol{x}) = \mathrm{T}_0 + \phi(\boldsymbol{x})$:

$$S_{\rm NC} = \theta \int \mathrm{d}^2\boldsymbol{x} \left[V_0 + \left(\lambda_4 \mathrm{T}_0^2 \phi^2 + \lambda_4 \mathrm{T}_0 \phi^3 + \frac{\lambda_4}{4}\phi^4 \right) + \left(-\frac{1}{2\theta} \left(\partial_{\boldsymbol{x}}\phi\right)^2 \right) \right]_\star . \tag{2.32}$$

Consider, for definiteness, the non-planar, one-loop contribution to the connected two-point Green function, depicted in Fig. 4. This diagram provides an example of IR problems in NCFT [21].

The contribution involves the following moduli-space integral associated with the one-loop Feynman diagram, where D denotes the spacetime dimension:

$$I_D = \int_0^\infty \mathrm{d}t \frac{1}{t^{D/2}} \exp\left(-tm^2 - \frac{\Lambda_{\rm eff}^2}{t} \right),$$

where $m^2 = 2$ from (2.32), $\boldsymbol{p}$ is the momentum flow through the external line, and

$$\Lambda_{\rm eff}^{-2} = \Lambda_{\rm UV}^{-2} + 2\lambda_4 \left(\theta\cdot\boldsymbol{p}\right)^2 .$$

The result is

$$\begin{aligned} I_2 \;&=\; 2K_0\left(2m/\Lambda_{\rm eff}\right) \to \log\left(2m/\Lambda_{\rm eff}\right) + \ldots \\ &\qquad\qquad \text{for}\;\; (2m/\Lambda_{\rm eff}) \ll 1 \\ &\to 2K_0\left(2m|\theta\boldsymbol{p}|\right) \quad \text{for} \quad \boldsymbol{p} = \text{finite}, \quad \Lambda \to \infty \\ &\sim 2K_0\left(2m\theta/L\right) \quad \text{for} \quad |\boldsymbol{p}| \sim 1/L. \end{aligned}$$

Using the relation $L = (\theta N)^{1/2}$ on $\mathbb{TT}^2_\theta$, we finally obtain

$$I_2 = 2K_0\left(\frac{2m}{g_{\rm eff}}\right). \tag{2.33}$$

Thus, $I_2 = \infty$ in the disordered phase, I_2 is finite in the planar phase, and $I_2 = 0$ in the GMS phase. This is exactly as we would predict on the basis of our earlier discussion of the behavior of the quantum effective action in the limits (1.2), namely that the GMS solution remains stable in the limit (a), has a finite correction in the planar limit (b), and is completely destabilized in the limit (c), where the measure term becomes infinitely large compared to the classical term in the action.

3 Effect of the gradient term

The foregoing discussion was largely based on keeping only the leading order term, $\mathcal{L}_0$ in (2.5), in the large θ limit. While the gradient term $\mathcal{L}_{-1}$ is of sub-leading order in $(1/\theta)$ expansion, as noted below (A.4), it breaks the $U(\infty)$ symmetry explicitly – a point which one ought to be concerned with for its consequential effects to the results we have obtained in the previous subsections. In particular, as the dramatic quantum effects we have deduced are largely based on the $\mathcal{L}_0$-term and the $U(\infty)$ symmetry therein, one might suspect that the term $\mathcal{L}_{-1}$, being part of the classical action, would render a sizable symmetry breaking effect. This is because the size of the gradient term is given by

$$\$_{-1} = \int \mathrm{d}^2\boldsymbol{x}\mathcal{L}_{-1} = \int \mathrm{d}^2\boldsymbol{x} \left(-\frac{1}{2}[\boldsymbol{x},\mathrm{T}]^2_\star \right) \sim \mathcal{O}(N^2).$$

Fortuitously, as we will show in this section, the gradient effect turns out to be of order $\mathcal{O}(N^2 g_{\rm eff}^2)$, viz. scales further by a factor of the 't Hooft coupling, $g_{\rm eff}^2$. The scaling is not universally valid, but only for $g_{\rm eff} < g_{\rm eff}^c$ for some finite $g_{\rm eff}^c$, as is inferred from the large-N phase transition [26]. As we are interested in the weak 't Hooft coupling regime, $g_{\rm eff} \ll 1$, the above counting holds valid. In particular, it implies that the measure effect, whose size is of order $\mathcal{O}(N^2)$, outweighs the gradient effect. Thus, in the weak 't Hooft coupling regime, one can utilize the $U(\infty)$ symmetry, and recast the NCFTs literally as the $N \to \infty$ limit of the matrix model studied in [15].

3.1 Perturbative estimates

We will begin, utilizing the Weyl formulation of the NCFT, with the computation of leading order perturbative corrections. For this purpose, we regularize the theory so that the fields are defined on N-dimensional Hilbert space, $\mathcal{H}_\theta[N]$, spanned by $\mathrm{Span}[|n\rangle, n = 0,\ldots,N-1]$, where

$$|n\rangle = \frac{a^{\dagger n}}{\sqrt{n!}}|0\rangle \quad \text{and} \quad \frac{1}{\sqrt{2}}\left[\widehat{\boldsymbol{x}^1} \pm \mathrm{i}\widehat{\boldsymbol{x}^2}\right] \equiv (\boldsymbol{a}, \boldsymbol{a}^\dagger).$$

Taking the potential to be (2.8) and expanding around $\boldsymbol{T} = 0$, the NCFT partition function (2.15) is given by[5]

$$\mathsf{Z}_N = \int [\mathrm{d}\boldsymbol{T}]_N \exp\left(-\$_{\rm NC}[\theta;\boldsymbol{T}]\right),$$

where

$$\$_{\rm NC} = (\$_{\rm cl} + \$_{\rm 0P} + \$_{\rm 0V}) + \$_{-1}.$$

[5] Actually, in (2.8), $\boldsymbol{T} = 0$ is an unstable point. One might alternatively expand the potential around stable vacua, $\boldsymbol{T} = \pm \mathrm{T}_0 \mathbb{I}$. This would give rise to an additional cubic interaction, but it turns out that the conclusion based on (3.1) remains unchanged

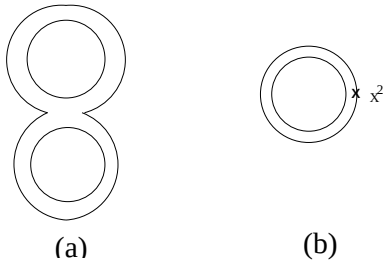

Fig. 5a,b. Feynman diagrams for leading order quantum corrections due to **a** the potential S_{0V}, and **b** the gradient term S_{-1}

Here

$$\begin{aligned}
\$_{\rm cl} &= \theta {\rm Tr} V(0), \quad \text{where} \quad V(0) = V_0 + \frac{\lambda_4}{4} {\rm T}_0^4, \\
\$_{0{\rm P}} &= \theta {\rm Tr}\left(\frac{m^2}{2}\boldsymbol{T}^2\right), \quad \text{where} \quad m^2 = \frac{\lambda_4}{2}{\rm T}_0^2, \\
\$_{0{\rm V}} &= \theta {\rm Tr}\left(\frac{\lambda_4}{4}\boldsymbol{T}^4\right), \\
\$_{-1} &= {\rm Tr}\left(-\frac{1}{2}\,[\widehat{\boldsymbol{x}}, \boldsymbol{T}]^2\right). \qquad (3.1)
\end{aligned}$$

3.2 Leading order corrections

The leading order quantum corrections to the free energy are obtained as

$$\begin{aligned}
\langle \$(\boldsymbol{T})\rangle_{0{\rm P}} &= \frac{1}{{\rm Z}_{0{\rm P}}}\int [{\rm d}\boldsymbol{T}]\$(\boldsymbol{T})\exp(-\$_{0{\rm P}}) \\
&= \$_{\rm cl} + \Delta\$_{0{\rm P}} + \Delta\$_{0{\rm V}} + \Delta\$_{-1} + \ldots \qquad (3.2)
\end{aligned}$$

where ${\rm Z}_{0{\rm P}} := \int [{\rm d}\boldsymbol{T}]\exp(-\$_{0{\rm P}})$ and

$$\begin{aligned}
\$_{\rm cl} &\equiv \theta {\rm Tr} V(0) \sim \theta N V(0), \\
\Delta\$_{0{\rm P}} &\equiv \theta m^2 \ \langle {\rm Tr}\boldsymbol{T}^2\rangle_{0{\rm P}} \sim N^2, \\
\Delta\$_{0{\rm V}} &\equiv \langle \$_{0{\rm V}}\rangle_{0{\rm P}} = \theta\lambda_4 \cdot \frac{N^3}{(\theta m^2)^2}, \\
\Delta\$_{-1} &\equiv \langle \$_{-1}\rangle_{0{\rm P}} = \frac{N\cdot N^2}{\theta m^2}. \qquad (3.3)
\end{aligned}$$

Diagrammatically, $\Delta\$_{0{\rm P}}$ originates from the one-loop vacuum diagram, while $\Delta\$_{0{\rm V}}$ and $\Delta\$_{-1}$ are from the diagrams (a) and (b) in Fig. 5, respectively. Note that the propagator is given by $\langle \boldsymbol{T}\boldsymbol{T}\rangle_{0{\rm P}} \sim 1/(\theta m^2)$. Thus, the diagrams are evaluated as follows. For diagram (a), the contribution equals (vertex) $[\theta\lambda_4]\times$ (two propagators) $[1/(\theta m^2)^2]\times$ (three "color" loops) $[N^3]$. In evaluating $\langle \$_{-1}\rangle_{0{\rm P}}$, the two terms will contribute ${\rm Tr}\,(\boldsymbol{T}\hat{\boldsymbol{x}}_a\boldsymbol{T}\hat{\boldsymbol{x}}_a)$ and ${\rm Tr}\left(\boldsymbol{T}^2\hat{\boldsymbol{x}}_a^2\right)$. As ${\rm Tr}\hat{\boldsymbol{x}}_a = 0$, only the latter will contribute, and it is given by Feynman diagram (b) in Fig. 5. There, X^2 on the outer color loop refers to the insertion of ${\rm Tr}\left(\widehat{\boldsymbol{x}}_a^2\right) \sim \sum_{n=0}^{N-1} n = \mathcal{O}(N^2)$. Hence, for diagram (b), the contribution equals (color loop) $[N]\times$ (color loop with X^2 insertion) $[N^2]\times$ (one propagator) $[1/(\theta m^2)]$.

To proceed, introduce the following rescaled parameters:

$$\overline{\lambda_4} := \frac{\lambda_4}{m^2}, \quad \overline{V}(0) := \frac{V(0)}{m^2}, \quad \overline{\theta} := \frac{m^2\theta}{N} = \frac{m^2}{g_{\rm eff}^2}.$$

Making in (3.1) a change of the variable $\theta m^2\boldsymbol{T}^2 = \boldsymbol{M}^2$ and bringing the quadratic term into a canonical normalization, we have

$$\begin{aligned}
\$_{\rm NC} = N^2\overline{\theta V}(0) + {\rm Tr}\Bigg[&\frac{1}{2}\boldsymbol{M}^2 + \frac{1}{N}\frac{\overline{\lambda_4}}{\overline{\theta}}\left(\frac{1}{4}\boldsymbol{M}^4\right) \\
&+ \frac{1}{N}\frac{1}{\overline{\theta}}\left(-\frac{1}{2}[\widehat{\boldsymbol{x}}_a, \boldsymbol{M}]^2\right)\Bigg], \qquad (3.4)
\end{aligned}$$

with which the partition function (2.18) can be defined. Equation (3.4) reveals that the effective coupling of the potential term is $(\overline{\lambda_4}/\overline{\theta})$ and that of the gradient term is $1/\overline{\theta}$. For the perturbation theory to make sense, one will need these couplings to be small enough. We now ask if there is a range of parameters satisfying this restriction as well as the condition that the gradient terms are suppressed compared to the potential term. There indeed does exist such a region in the space of the rescaled parameters, viz.

$$\overline{\theta} \gg \overline{\lambda_4} \gg 1. \qquad (3.5)$$

The first limit, $\overline{\theta} \gg 1$, is readily attainable, in the non-commutative torus regularization adopted in (2.13), by taking $n \sim \mathcal{O}(N)$. We will now explicitly verify that, in this weak coupling regime, the gradient term is suppressed, at least at leading order in the perturbation theory. In terms of the rescaled parameters, the estimates (3.3) are re-expressible as

$$\begin{aligned}
&\$_{\rm cl} = N^2\overline{\theta V}(0), \quad \Delta\$_{0{\rm P}} = N^2, \quad \Delta\$_{0{\rm V}} = N^2\left(\frac{\overline{\lambda_4}}{\overline{\theta}}\right), \\
&\Delta\$_{-1} = N^2\left(\frac{1}{\overline{\theta}}\right). \qquad (3.6)
\end{aligned}$$

We thus realize that, in the 't Hooft's large-N limit, all the terms are of order $\mathcal{O}(N^2)$, and hence are planar. However, the weak coupling limit ensures that the leading order corrections are hierarchically ordered:

$$\$_{\rm cl} \gg \Delta\$_0 \gg \Delta\$_1 \gg \Delta\$_{-1}. \qquad (3.7)$$

Hence, we conclude that, under (3.5), the gradient term $\$_{-1}$ is indeed suppressed compared to the potential term.

3.3 Higher order corrections

To ensure that the scaling limit (3.5) is sufficient for dropping the gradient terms at least perturbatively, we now evaluate next-to-leading order corrections. These arise from the second order expansion of the partition function, and are given by the connected vacuum diagrams, see Fig. 7:

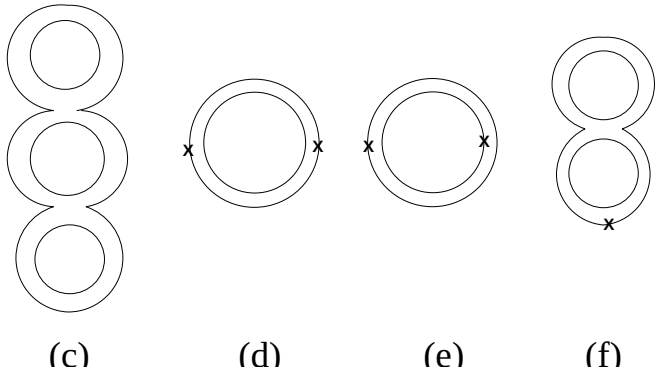

Fig. 6c–f. Feynman diagrams for higher order quantum corrections due to **c** the potential $(S_{0V})^2$, **d** and **e** the gradient terms $(S_{-1})^2$, and **f** the cross term $(S_{0V}S_{-1})$

$$\left\langle \frac{1}{2!}\$^2 \right\rangle_{0P}^{\text{conn}} = \frac{1}{\mathsf{Z}_{0P}} \int_{\text{connected}} [\mathrm{d}\boldsymbol{M}] \frac{1}{2!} \left(\$_{0V} + \$_{-1}\right)^2 \times \exp\left(-\$_{0P}\right).$$

Dropping again "dimensionless" numerical factors of $\mathcal{O}(1)$, we obtain the corrections as follows:

$$\begin{aligned}
&\text{diagram (c)} \sim (\theta\lambda_4)^2 \frac{N^4}{(\theta m^2)^3} = N^2 \left(\frac{\overline{\lambda_4}}{\overline{\theta}}\right)^2, \\
&\text{diagram (d)} \sim \quad \frac{N\cdot N^3}{(\theta m^2)^2} \quad = N^2 \left(\frac{1}{\overline{\theta}}\right)^2, \\
&\text{diagram (e)} \sim \quad \frac{N^2\cdot N^2}{(\theta m^2)^2} \quad = N^2 \left(\frac{1}{\overline{\theta}}\right)^2, \\
&\text{diagram (f)} \sim (\theta\lambda_4)\frac{N\cdot N\cdot N^2}{(\theta m^2)^3} = N^2 \left(\frac{\overline{\lambda_4}}{\overline{\theta}}\right). \qquad (3.8)
\end{aligned}$$

Evidently, the insertion of the gradient term $\$_{-1}$ is accompanied by an extra factor of $\overline{\lambda}_4/\overline{\theta}$. In the scaling limit (3.5), the factor is small enough. We thus conclude that, by taking the scaling limit (3.5), the effect of the gradient terms can be made hierarchically small compared to the Vandermonde effect.

3.4 Non-perturbative estimate

We will now make use of Feynman's variational method [27,28], and prove non-perturbatively that the scaling limit (3.5) ensures subdominance of the gradient terms. From (2.19) expressed in terms of the rescaled action (3.4),

$$\begin{aligned}
\mathsf{Z}_N &:= \exp(-F_{\text{exact}}) \\
&= \int [\mathrm{d}\boldsymbol{M}] \exp(-\$_0) \exp(-\$_{-1}) \\
&= \int [\mathrm{d}\boldsymbol{M}] \exp(-\$_0) \left\langle \exp(-\$_{-1}) \right\rangle_0,
\end{aligned}$$

where F_{exact} refers to the exact free energy, $\$_0 = (\$_{0P} + \$_{0V})$, and

$$\langle \cdots \rangle_0 := \int [\mathrm{d}\boldsymbol{M}] \cdots \exp(-\$_0) / \int [\mathrm{d}\boldsymbol{M}] \exp(-\$_0).$$

Applying Jensen's inequality, we have

$$\mathsf{Z}_N \geq \int \prod_{a=1}^{N} [\mathrm{d}\boldsymbol{M}] \exp(-\$_0) \exp\left(-\left\langle \$_{-1} \right\rangle_0\right).$$

Thus, we find a variational estimate to the upper bound of the exact free energy:

$$F_{\text{exact}} \leq F_0 + \Delta F,$$

where

$$F_0 = -\ln \int [\mathrm{d}\boldsymbol{M}] \exp(-\$_0) \quad \text{and} \quad \Delta F := \left\langle \$_{-1} \right\rangle_0. \qquad (3.9)$$

The quantity ΔF can be evaluated explicitly by utilizing the well-known formula [29]

$$\langle \boldsymbol{M}_{kl} \boldsymbol{M}_{mn} \rangle_0 = C_1 \delta_{kl}\delta_{mn} + C_2 \delta_{kn}\delta_{lm}, \qquad (3.10)$$

where

$$C_1 = \frac{\left\langle (\mathrm{Tr}\boldsymbol{M})^2 \right\rangle_0}{(N^2-1)} - \frac{\left\langle \mathrm{Tr}\boldsymbol{M}^2 \right\rangle_0}{N(N^2-1)}$$

and

$$C_2 = \frac{\left\langle \mathrm{Tr}\boldsymbol{M}^2 \right\rangle_0}{(N^2-1)} - \frac{\left\langle (\mathrm{Tr}\boldsymbol{M})^2 \right\rangle_0}{N(N^2-1)}.$$

Equation (3.10) can be proved from the $U_{\mathrm{L}}(N) \times U_{\mathrm{R}}(N)$ invariance of both the action $\$_0$ and the integral measure $[\mathrm{d}\boldsymbol{M}]$. Hence, the correction ΔF in (3.9) is computed to be

$$\begin{aligned}
\Delta F &= \left\langle \frac{1}{\overline{\theta}} \frac{1}{N} \mathrm{Tr} \left(-\frac{1}{2} [\widehat{\boldsymbol{x}}^a, \boldsymbol{M}]^2 \right) \right\rangle \\
&= \frac{1}{\overline{\theta}} \left[-\left(\widehat{\boldsymbol{x}}^a_{nk} \widehat{\boldsymbol{x}}^a_{lm}\right) \frac{1}{N} \left\langle \boldsymbol{M}_{kl} \boldsymbol{M}_{mn} \right\rangle_0 \right. \\
&\qquad \left. + \left(\widehat{\boldsymbol{x}}^a \widehat{\boldsymbol{x}}^a\right)_{nk} \frac{1}{N} \left\langle (\boldsymbol{M}^2)_{kn} \right\rangle_0 \right] \\
&= \left[\frac{1}{N(N^2-1)} \Big(N \left\langle \mathrm{Tr}\boldsymbol{M}^2 \right\rangle_0 \right. \\
&\qquad \left. - \left\langle (\mathrm{Tr}\boldsymbol{M})^2 \right\rangle_0 \Big) \right] \frac{1}{\overline{\theta}} \mathrm{Tr}(\widehat{\boldsymbol{x}}^a \widehat{\boldsymbol{x}}^a),
\end{aligned}$$

where, in the last equality, we have used the fact that $\mathrm{Tr}\boldsymbol{x}^a = 0$. Evidently, from the last expression, as $\left\langle \mathrm{Tr}\boldsymbol{M}^2 \right\rangle$ and $\left\langle (\mathrm{Tr}\boldsymbol{M})^2 \right\rangle$ scale with N as $\mathcal{O}(N^2)$, the coefficients inside the square bracket are of order $\mathcal{O}(1)$. Hence, ΔF is proportional to $\mathrm{Tr}(\widehat{\boldsymbol{x}}^a \widehat{\boldsymbol{x}}^a)/\overline{\theta}$, and is of order $\mathcal{O}(N^2/\overline{\theta})$. As the $\$_{\text{classial}}$ and $\langle \$_0 \rangle$ scale as $\mathcal{O}(N^2\overline{\theta})$ and $\mathcal{O}(N^2)$, respectively, the above estimate indeed shows that the gradient term contribution is bounded from above to a value suppressed by powers of $1/\overline{\theta}$. This completes the proof that (3.7) holds at the non-perturbative level.

3.5 Remarks on gradients in gauge theories

In case the NCFT is promoted to gauge theories, the situation becomes even more favorable. In this section, we have also restricted our investigation to NCFTs consisting only of scalar fields – corresponding to the level-zero truncation in the context of open string field theory. Once the gauge field is coupled, the action is schematically given by

$$S_{\rm NC} = \int_{\mathbb{R}^2} \mathrm{d}^2\boldsymbol{y} \left[\frac{1}{4} F_{mn} \star_\theta F_{mn} + \frac{1}{2} D_m(A)\mathrm{T} \star_\theta D_m(A)\mathrm{T} + V_{\star_\theta}(\mathrm{T}) + \cdots \right],$$

corresponding to truncation of the open string field theory at level one. Here, $D_m(A)\mathrm{T} := \partial_m \mathrm{T} + [A_m, \mathrm{T}]_\star$, and, via the Weyl–Moyal map, it is expressible as proportional to $[\boldsymbol{Y}_m, \mathrm{T}]$, where $\boldsymbol{Y}^m := \boldsymbol{y}^m + \theta^{mn} A_n(\boldsymbol{y})$. A crucial observation for the present discussion is that, as the authors of [4] have pointed out, $\boldsymbol{Y}^m = 0$ in classical vacua at any non-zero value of θ. Because of this, the tachyon gradient term, $[\boldsymbol{Y}_m, \boldsymbol{T}]^2$, drops out of the Euclidean action completely. Moreover, this nullification takes place for a finite value of θ.

4 $D = (2+1)$ non-commutative field theories

We next turn our attention to non-commutative field theories in $(2+1)$-dimensional spacetime. As in the previous sections, our main motivation for these theories would be that these theories describe tachyon dynamics on an unstable D2-brane, either in bosonic or in Type IIB superstring theories, at non-zero B-field background. The main result we shall be showing is that, at low-energy, *quantum* aspects of vacua and solitons (corresponding to non-BPS D0-branes) are governed by *quantum mechanics* of a $(0+1)$-dimensional Hermitian matrix model. Moreover, we again find that the continuum and semiclassical limit is governed by the large-N, large-θ limit. Most of the discussions are closely parallel to the two-dimensional case of the previous section. Nevertheless, for the sake of the readers, we will repeat those parts relevant for foregoing discussions.

4.1 Classical theory

Let us begin with the non-commutative $(2+1)$-dimensional spacetime $\mathbb{R}^{2,1}_\theta$ whose coordinates are $(t, \boldsymbol{y})$ and with "spacelike" non-commutativity θ^{ab}:

$$\left[y^a, y^b\right] = \mathrm{i}\theta^{ab} \quad \text{and} \quad [t, y^a] = 0, \quad (a, b = 1, 2).$$

Take a field theory on $\mathbb{R}^{2,1}_\theta$, consisting of a scalar field $\mathrm{T}(t, \boldsymbol{y})$ with self-interaction potential $V(\mathrm{T})$. The Seiberg–Witten map enables us to map the theory into to a non-commutative field theory on $\mathbb{R}^{2,1}$, whose action is given by

$$S_{\rm NC}[\theta; \mathrm{V}] = \int_{\mathbb{R}^{2,1}} \mathrm{d}t\mathrm{d}^2\boldsymbol{y} \left[\frac{1}{2}\partial_t \mathrm{T} \star_\theta \partial_t \mathrm{T} - \frac{1}{2}\partial_{\boldsymbol{y}} \mathrm{T} \star_\theta \partial_{\boldsymbol{y}} \mathrm{T} - V_\star(\mathrm{T}) \right]. \tag{4.1}$$

The non-commutativity θ^{ab} is encoded into the $\star_\theta$-product, defined as before; see (2.3). We are again interested in the large non-commutativity limit, $\theta \to \infty$. Rescale the spatial coordinates, $\boldsymbol{y} \to \boldsymbol{x}$, the same way as in (2.4), and expand the action (4.1) in powers of $(1/\theta)$:

$$S_{\rm NC}[\theta; V] = \theta \int_{\mathbb{R}^{2,1}} \mathrm{d}t\mathrm{d}^2\boldsymbol{y} \left[\mathcal{L}_0 + \frac{1}{\theta}\mathcal{L}_{-1} + \cdots \right], \tag{4.2}$$

where

$$\mathcal{L}_0 = \frac{1}{2}\left((\partial_t \mathrm{T})^2 - V_\star(\mathrm{T}) \right) \quad \text{and} \quad \mathcal{L}_{-1} = -\frac{1}{2}(\partial_{\boldsymbol{x}} \mathrm{T})^2.$$

Again, for large non-commutativity, $(1/\theta) \to \infty$, the gradient term $\mathcal{L}_{-1}$ drops out.

The aforementioned Weyl–Moyal map,

$$\mathrm{T}(\boldsymbol{x}, t) = \int_{\widetilde{\mathbb{R}^2}} \frac{\mathrm{d}^2\boldsymbol{k}}{(2\pi)^2} \mathrm{Tr}_{\mathcal{H}} \left(\mathrm{e}^{\mathrm{i}\boldsymbol{k}\cdot\widehat{\boldsymbol{x}}} \boldsymbol{T}(t) \right) \mathrm{e}^{-\mathrm{i}\boldsymbol{k}\cdot\boldsymbol{x}},$$

then permits us to re-express the $(2+1)$-dimensional NCFT (4.2) as a one-dimensional Hermitian matrix model:

$$\$_{\rm NC}[\theta; V] = \theta \int \mathrm{d}t \mathrm{Tr}_{\mathcal{H}} \left[\left(\frac{1}{2}(\partial_t \boldsymbol{T})^2 - V(\boldsymbol{T}) \right) + \frac{1}{\theta}\left(+\frac{1}{2}[\hat{\boldsymbol{x}}, \boldsymbol{T}]^2 \right) + \cdots \right]. \tag{4.3}$$

At leading order in $(1/\theta)$, both (4.2) and (4.3) are invariant under the $U(\infty)$ symmetry group of area-preserving diffeomorphisms:

$$\begin{aligned} \mathrm{T}(\boldsymbol{x}, t) \;&\to\; U(\boldsymbol{x}, t) \star \mathrm{T}(\boldsymbol{x}, t) \star U^{-1}(\boldsymbol{x}, t) \\ &\longleftrightarrow \boldsymbol{T} \to \boldsymbol{U}(t)\boldsymbol{T}(t)\boldsymbol{U}^{-1}(t). \end{aligned}$$

The scalar field, realized as an operator field $\boldsymbol{T}(t)$ on the auxiliary Hilbert space $\mathcal{H}$, is expandable as a linear combination of one-dimensional projection operators:

$$\boldsymbol{T}(t) = \sum_{\ell=1}^{\dim\mathcal{H}} \lambda_{a_\ell}(t) \boldsymbol{P}_\ell,$$

where the one-dimensional projection operators $\boldsymbol{P}_\ell$ are defined as in (A.3) and the coefficients λ_a are generically time-dependent.

4.2 Classical vacua and solitons

Utilizing the one-dimensional projection operators $\boldsymbol{P}_\ell$, it is straightforward to construct *static* classical solutions, as shown first in [3]. Denote the critical points of the potential, defined by $V'(\lambda) = 0$, as $\lambda_0, \lambda_1, \lambda_2, \cdots$, arranged

in ascending order of the critical point energy: $V(\lambda_0) \leq V(\lambda_1) \leq V(\lambda_2) \leq \cdots$ The most general solution to the tachyon equation of motion

$$-\partial_t^2 \boldsymbol{T}(t) - V'(\boldsymbol{T}) = 0$$

is expressible as

$$\boldsymbol{T}(0) = \sum_{\ell=1}^{\dim\mathcal{H}} \lambda_{a_\ell} \boldsymbol{P}_\ell,$$

where the coefficients $\lambda_{a_\ell}(t)$ obeys the single-particle equation of motion

$$-\ddot{\lambda}_{a_\ell}(t) - V'(\lambda_{a_\ell}(t)) = 0.$$

Evidently, the ath vacuum is given by

$$\boldsymbol{T}_a = \sum_{\ell=1}^{\dim\mathcal{H}} \lambda_a \boldsymbol{P}_\ell = \lambda_a \mathbb{I}_{\mathcal{H}} \quad (a = 0, 1, 2, \cdots),$$

where the λ_{a_ℓ} take values out of the set $(\lambda_0, \lambda_1, \cdots)$ permitting duplications. Likewise, a classical static soliton is given by

$$\boldsymbol{T}_{\text{soliton}}(t) = \sum_{\ell=1}^{\dim\mathcal{H}} \lambda_\ell \boldsymbol{P}_\ell,$$

where the coefficients λ_ℓ consist of *at least* two distinct values among the critical points. For example, a static soliton of type (N_a, N_b) is given by

$$\boldsymbol{T}_{(N_a,N_b)} = \lambda_a \boldsymbol{P}_{[N_a]} + \lambda_b \boldsymbol{P}_{[N_b]}. \tag{4.4}$$

Not surprisingly, the soliton takes the same form as the $[N_a, N_b]$ instanton considered in Sect. 2, as, even in a non-commutative context, instantons in $(2+0)$-dimensional NCFT are identifiable with static configuration of solitons in $(2+1)$-dimensional NCFT.

To exemplify this, consider again the symmetric double-well potential:

$$V(\boldsymbol{T}) = V_0 + \frac{\lambda_4}{4}\left(\boldsymbol{T}^2 - \mathrm{T}_0^2\right)^2.$$

The classical vacua are given by the linear operators

$$\boldsymbol{T}_{\text{vacuum}} = \pm \mathrm{T}_0 \mathbb{I},$$

while the static (N_1, N_2) soliton is given by

$$\boldsymbol{T}_{N_1,N_2} = \mathrm{T}_0 \left(\boldsymbol{P}_{[N_1]} - \boldsymbol{P}_{[N_2]}\right).$$

The $U(\infty)$ invariant collective excitations are encoded into the eigenvalue density field $\rho(\lambda, t)$ [30]:

$$\rho(\lambda, t) := \frac{1}{\dim\mathcal{H}} \sum_{\ell=1}^{\dim\mathcal{H}} \delta(\lambda - \lambda_\ell(t)). \tag{4.5}$$

For example, the static (N_1, N_2) soliton is then given by a saddle-point configuration of the density field $\rho_{\mathrm{s}}(\lambda)$:

$$\rho_{[N_1,N_2]}(\lambda) = n_1 \delta(\lambda - \mathrm{T}_0) + n_2 \delta(\lambda + \mathrm{T}_0),$$

where

$$n_{1,2} = \frac{N_{1,2}}{\dim\mathcal{H}}. \tag{4.6}$$

4.3 Quantum theory

Definition

For the definition of the theory at the quantum level, we will adopt the same prescription as for the $(2+0)$-dimensional case. Thus, in the Moyal formulation via $(2+1)$-dimensional NCFT, the *regularized* partition function is defined by

$$\mathcal{Z}_{\mathrm{NC}}[\theta, V_\star; L_1 L_2] = \int [\mathrm{dT}(t)]_{L_1,L_2} \exp(-S_{\mathrm{NC}}[\theta; V_\star(\mathrm{T})]).$$

In the Weyl formulation via the $(0+1)$-dimensional Hermitian matrix model, the *regularized* partition function is defined by

$$\mathsf{Z}_N[\theta, V; N] = \int [\mathrm{d}\boldsymbol{T}(t)]_N \exp\left(-\$_{\mathrm{NC}}[\theta; V(\boldsymbol{T})]\right),$$

where the integration measure is defined as in $(2+0)$-dimensional NCFT:

$$[\mathrm{dT}]_N := \prod_{-\infty<t<+\infty} \left(\prod_{\ell=1}^{N} \mathrm{dT}_{\ell\ell}(t) \prod_{1\leq\ell<m\leq N} 2\mathrm{dReT}_{\ell m}(t)\mathrm{ImT}_{\ell m}(t) \right). \tag{4.7}$$

The Weyl–Moyal correspondence then implies that

$$\lim_{L_1 L_2 \to \infty} \mathcal{Z}_{\mathrm{NC}}[\theta, V_\star; L_1 L_2] \quad \equiv \lim_{N\to\infty} \mathsf{Z}_N[\theta, V; N].$$

We will thus investigate the quantum effects in terms of the right-hand side, viz. the $(0+1)$-dimensional Hermitian matrix model. We are interested in computing the ground-state energy and low-energy excitations of the theory. From (2.6) and the definition of the integration measure (4.7), one readily obtains the Hamiltonian:

$$\mathsf{H} = -\frac{1}{2\theta} \Delta_{\boldsymbol{T}} + \theta \mathrm{Tr} V(\boldsymbol{T}) + \Delta\mathsf{H}_{\mathrm{grad}},$$

where

$$\begin{aligned} \Delta_{\boldsymbol{T}} &:= -\mathrm{Tr}\Pi_{\boldsymbol{T}}^2 = \sum_{\ell=1}^{N} \frac{\partial^2}{\partial \boldsymbol{T}_{\ell\ell}^2} \\ &\quad + \frac{1}{2} \sum_{1\leq\ell<m\leq N} \left(\frac{\partial^2}{\partial \mathrm{Re}\boldsymbol{T}_{\ell m}^2} + \frac{\partial^2}{\partial \mathrm{Im}\boldsymbol{T}_{\ell m}^2} \right) \\ \Delta\mathsf{H}_{\mathrm{grad}} &= \left(-\frac{1}{2} [\widehat{\boldsymbol{x}}, \boldsymbol{T}] \right)^2. \end{aligned} \tag{4.8}$$

For now, anticipating a similar power-counting suppression as in the two-dimensional NCFTs, we will drop the gradient term $\Delta\mathsf{H}_{\mathrm{grad}}$, and justify it later in Sect. 4.5. Parametrize the matrix field $\boldsymbol{T}(t)$ as

$$\boldsymbol{T}(t) = \boldsymbol{U}(t) \cdot \boldsymbol{T}_{\mathrm{d}}(t) \cdot \boldsymbol{U}^{-1}(t),$$

where

$$\boldsymbol{T}_{\mathrm{d}}(t) = \mathrm{diag.}\left(\lambda_1(t), \cdots, \lambda_N(t)\right).$$

The "angular" matrix $\boldsymbol{U}(t)$ parametrizes the coset space $SU(N)/\mathcal{W}$, where $\mathcal{W}$ refers to the Weyl group, permuting the eigenvalues. Evidently, as the Hamiltonian is invariant under the $U(\infty)$ transformation, the ground-state wave function $\Psi(\boldsymbol{T})$ ought to be a symmetric function of the eigenvalues λ_ℓ of $\boldsymbol{T}$. The ground-state energy is given by

$$E_{\text{g.s.}} = \lim_{N\to\infty} \text{Min}_\Psi \frac{\langle\Psi|\mathsf{H}|\Psi\rangle}{\langle\Psi|\Psi\rangle}$$

over the variational wave functions Ψ. Here, the matrix elements are

$$\langle\Psi|\mathsf{H}|\Psi\rangle = \int [\mathrm{d}\boldsymbol{T}]\Psi^\dagger(\lambda)\mathsf{H}\Psi(\lambda)$$

and

$$\langle\Psi|\Psi\rangle = \int [\mathrm{d}\boldsymbol{T}]\Psi^\dagger(\lambda)\Psi(\lambda).$$

Note that the ground-state wave function Ψ is invariant under the transformation $\boldsymbol{T}(t) \to \boldsymbol{U}(t)\boldsymbol{T}(t)\boldsymbol{U}^{-1}(t)$. Eliminating the "angular" variables $\boldsymbol{U}(t)$, the matrix elements can be rewritten as

$$\begin{aligned}\langle\Psi|\mathsf{H}|\Psi\rangle &= \int \prod_{\ell=1}^N \mathrm{d}\lambda_\ell \Delta^2(\lambda) \\ &\quad\times \left(\frac{1}{2}\sum_{\ell=1}^N |\partial_{\lambda_\ell}\Psi(\lambda)|^2 + V(\lambda)\,|\Psi(\lambda)|^2\right), \\ \langle\Psi|\Psi\rangle &= \int \prod_{\ell=1}^N \mathrm{d}\lambda_\ell \Delta^2(\lambda)\,|\Psi(\lambda)|^2;\end{aligned}$$

the Vandermonde determinant $\Delta(\lambda) = \prod_{\ell<m}(\lambda_\ell - \lambda_m)$ arises as the Jacobian of the change of variables, (4.9). The expression suggests the introduction of an *antisymmetric* wave function $\Phi(\lambda)$:

$$\Phi(\lambda) = \Delta(\lambda)\Psi(\lambda_1, \cdots, \lambda_N)$$

as the wave function of $N := \dim\mathcal{H}$ species of the first-quantized "analog" *fermions* in one dimension, spanned by the eigenvalues. The corresponding Schrödinger equation is given by

$$\mathrm{i}\frac{\partial}{\partial t}\Phi(\lambda_1, \cdots, \lambda_N; t) = \mathsf{H}_{\text{NC}}\Phi(\lambda_1, \cdots, \lambda_N; t).$$

where the Hamiltonian H_{NC} is given by

$$\mathsf{H}_{\text{NC}} = \sum_{\ell=1}^N \mathcal{H}[\lambda_\ell]$$

as a sum of one-particle Hamiltonians $\mathcal{H}[\lambda]$

$$\mathcal{H}[\lambda] := \left[-\frac{1}{2\theta}\frac{\partial^2}{\partial\lambda^2} + \theta V(\lambda)\right]. \tag{4.9}$$

The Hamiltonian describes a non-interacting Fermi gas in an external potential $V(\lambda)$. The above Hamiltonian is precisely the one derivable from the action (4.3), but in terms of the diagonal field variables:

$$S = \theta\int \mathrm{d}t \sum_{\ell=1}^N \left[\frac{1}{2}(\partial_t\lambda_\ell)^2 - V(\lambda_\ell)\right].$$

4.4 Classical, planar, and disordered phases of NCFT$_3$

To explore possible disordered phases of the theory, we investigate what sort of vacuum structure emerges once quantum effects due to the many-body "analog" fermions are taken into account.

For concreteness, consider a potential $V(\lambda)$ with a unique minimum at $\lambda = 0$ whose classical vacuum is given by $\lambda_\ell = 0$ for *all* $\ell = 1, 2, \cdots, N$. A harmonic fluctuation around the vacuum is described by the action

$$S_{\text{harm}} = \theta\int \mathrm{d}t \sum_{\ell=1}^N \left[\frac{1}{2}(\partial_t\lambda_\ell)^2 - \left(V_0 + \frac{1}{2}\Omega^2\lambda_\ell^2 + \cdots\right)\right],$$

where $\Omega^2 := V''(\lambda = 0)$, and the Hamiltonian is

$$H_{\text{harm}} = \sum_{\ell=1}^N \left[\frac{1}{2\theta}\Pi_\ell^2 + \theta\left(V_0 + \frac{1}{2}\Omega^2\lambda_\ell^2\right)\right].$$

At classical level, the ground-state energy of the vacuum $\lambda = 0$ is given by $N\theta V_0$ and hence, assuming that V_0 is fixed, is of order $\mathcal{O}(N\theta)$. Quantum mechanically, the ground-state energy is increased by zero-point fluctuations, and is readily estimated by applying the Schwarz inequality:

$$\begin{aligned}\langle H\rangle &\gtrsim N\theta V_0 + \sum_{\ell=1}^N \left\langle \frac{\Pi_\ell}{\sqrt{2\theta}}\cdot\sqrt{\frac{\theta}{2}}\Omega\lambda_\ell\right\rangle \\ &\sim N\theta V_0 + \frac{1}{2}N\Omega.\end{aligned} \tag{4.10}$$

The last formula indicates that the quantum effect is of order $\mathcal{O}(N)$. One might be content that the result is consistent with what one anticipates from the following heuristic argument: for a harmonic fluctuation, the relevant degrees of freedom are the eigenvalues, $\lambda_\ell(t)$. As there are N eigenvalues, the zero-point fluctuation is estimated simply to be $N\cdot(1/2)\Omega$ and is of order $\mathcal{O}(N)$. If this reasoning is correct, then it implies that, for large non-commutativity $\theta \gg 1$, the quantum effects would be completely negligible, in sharp contrast to the $(2+0)$-dimensional case.

It turns out that the above reasoning is incorrect, as Fermi statistics of the "analog" fermions are not properly taken into account. We will argue momentarily that the quantum effect on the ground-state energy is of order $\mathcal{O}(N^2)$ and, based on this, the *quantum* NCFT comprises three distinct phases:

$$\begin{aligned}\text{classical GMS phase}: &\quad \theta \sim N^{1+\nu} \quad (\nu > 0), \\ \text{planar }'\text{tHooft phase}: &\quad \theta \sim N, \quad g_{\text{eff}}^2 = \text{fixed}, \\ \text{disordered phase}: &\quad \theta \sim N^{1-\nu} \quad (\nu > 0).\end{aligned} \tag{4.11}$$

To see these phases, it is sufficient to examine the ground-state energy at quantum vacua. For simplicity, we will approximate the potential by a quadratic function with $\Omega = 1$. Denoting the one-particle fermion energy levels by $e_1 \le e_2 \le e_3 \le \cdots$ and the Fermi energy by $e_{\rm F}$, the particle number N and the total energy $\mathcal{E}$ is given by [15]

$$\begin{aligned} N &:= \sum_{\ell=1} \theta\left(e_{\rm F} - e_\ell\right) \\ &= \int \frac{{\rm d}\lambda {\rm d}p}{2\pi} \Theta\left(e_{\rm F} - \frac{p^2}{2\theta} - \frac{1}{2}\theta\lambda^2 - \theta V_0\right), \\ \mathcal{E} &:= \sum_{\ell=1} e_\ell \Theta\left(e_{\rm F} - e_\ell\right) \\ &= \int \frac{{\rm d}\lambda {\rm d}p}{2\pi} \Theta\left(e_{\rm F} - \frac{p^2}{2\theta} - \frac{1}{2}\theta\lambda^2 - \theta V_0\right) \\ &\times \left[\frac{p^2}{2\theta} + \frac{1}{2}\theta\lambda^2 + \theta V_0\right]. \end{aligned}$$

Here, V_0 refers to the minimum of the potential, the *classical* energy.

The above expressions implies that, in the total energy $\mathcal{E}$, the classical contribution is of order $\mathcal{O}(N\theta)$, while the quantum contribution is of order $\mathcal{O}(N^2)$. To show this, solve first the Θ function constraint of the "Fermi surface" as

$$|p(\lambda)| \le \sqrt{2\theta}\sqrt{\widetilde{e_{\rm F}} - \frac{1}{2}\theta\lambda^2} \quad \text{where} \quad \widetilde{e_{\rm F}} := (e_{\rm F} - \theta V_0)\,.$$

It then allows one to compute N and $\mathcal{E}$ explicitly. Begin with the particle number, N. Integrating over p first, elementary algebra yields

$$\begin{aligned} N &= 2\int \frac{{\rm d}\lambda}{2\pi}\sqrt{2\theta}\sqrt{\widetilde{e_{\rm F}} - \frac{1}{2}\theta\lambda^2} \\ &= \widetilde{e_{\rm F}}. \end{aligned}$$

This indicates that the Fermi energy $\widetilde{e_{\rm F}} = (e_{\rm F} - \theta V_0)$ is of order $\mathcal{O}(N)$. We will thus set $\widetilde{e_{\rm F}} := N\widetilde{\epsilon}$ and, in the large-N limit, hold $\widetilde{\epsilon}$ fixed to $\mathcal{O}(1)$ constant. Similarly, integrating over p first, the total energy $\mathcal{E}$ is obtained as a sum of classical and quantum contributions:

$$\mathcal{E} = \mathcal{E}_{\rm classical} + \mathcal{E}_{\rm quantum},$$

where

$$\mathcal{E}_{\rm classical} = \widetilde{e_{\rm F}}\theta V_0 = \mathcal{O}(N\theta) \tag{4.12}$$

and

$$\mathcal{E}_{\rm quantum} = \left(\frac{1}{4} + \frac{1}{4}\right)\widetilde{e_{\rm F}}^2 = \frac{1}{2}\widetilde{e_{\rm F}}^2 = \mathcal{O}(N^2). \tag{4.13}$$

The first and the second terms in $\mathcal{E}_{\rm quantum}$ are the contributions of the kinetic and potential energies, respectively. Evidently, the result exhibits that $\mathcal{E}_{\rm quantum}$ is of order $\mathcal{O}(N^2)$, not $\mathcal{O}(N)$ as anticipated from the aforementioned naive reasoning. With Fermi statistics taken into account, this correct result can be understood intuitively as follows. In the $\theta \to \infty$ limit, the effect of the functional integral measure is to turn the eigenvalues into positions of the "analog" *fermions*. As such, because of the Fermi pressure, the ground-state energy will increase, with size estimated to be

$$\Delta\mathcal{E} \sim \sum_{\ell=0}^{N} \frac{1}{2}\ell\Omega \sim \mathcal{O}(N^2),$$

thus obtaining the correct scaling in the large-N limit.

From (4.12) and (4.13), we come to the conclusion that, in the large-N and large-θ limit, depending on the relative magnitude of N and θ, the ground-state energy will scale differently. If $N \gg \theta$, the ground-state energy is dominated by the classical contribution, which we have referred as the "classical phase". If $N \sim \theta$, the classical and the quantum contributions are equally important. This is the "planar phase" – the phase familiar in the context of the planar expansion of matrix models. If $N \ll \theta$, the energy is dominated by the quantum contribution, which we referred to as the "disordered phase".

4.5 Effects of the gradients

So far, our analysis was based on truncation of the $\Delta\mathsf{H}_{\rm gradient}$ term in (4.8). In this section, we will prove that this gradient term effect is negligible in the weak 't Hooft coupling regime, quite analogous to the situation for two-dimensional NCFTs analyzed in Sect. 3. For the present case, now dealing with temporal evolution, we will proceed slightly differently and utilize the Gibbs inequality (see, for example, [28]). Let us begin with the Euclidean partition function, expressed in terms of the canonically normalized field $\boldsymbol{M}(t) = \theta^{1/2}\boldsymbol{T}$:

$$\begin{aligned} \mathsf{Z}_N = \int [{\rm d}\boldsymbol{M}(t){\rm d}\boldsymbol{\Pi}(t)]_N \\ \times \exp\left(-\int \left[-{\rm i}{\rm Tr}\boldsymbol{\Pi}(t)\dot{\boldsymbol{M}}(t) + \mathsf{H}(\boldsymbol{M}(t))\right]{\rm d}t\right). \end{aligned} \tag{4.14}$$

Here, the Hamiltonian H is given by (4.8), which we decompose as

$$\mathsf{H} = \mathsf{H}_0 + \Delta\mathsf{H}_{\rm grad},$$

where

$$\begin{aligned} \mathsf{H}_0 &= \frac{1}{2}{\rm Tr}\Pi^2(t) + \frac{m^2}{2}{\rm Tr}\boldsymbol{M}^2, \\ \Delta\mathsf{H}_{\rm grad} &= \frac{1}{\theta}{\rm Tr}\left(-\frac{1}{2}\left[\widehat{\boldsymbol{x}}_a, \boldsymbol{M}\right]^2\right). \end{aligned} \tag{4.15}$$

The decomposition allows us to estimate the gradient effect non-perturbatively. To this end, we will apply the Gibbs inequality to the partition function (4.14), and obtain the following upper bound to the exact effective action $\Gamma_{\rm exact}$:

$$\Gamma_{\rm exact} \le \Gamma_0 + \Delta\Gamma.$$

Here,

$$\begin{aligned} \mathit{\Gamma}_0 &= -\ln \int [\mathrm{d}\boldsymbol{M}(t)\mathrm{d}\boldsymbol{\Pi}(t)]_N \\ &\quad \times \exp\left(-\int [-\mathrm{i}\mathrm{Tr}\mathit{\Pi}(t)\dot{\boldsymbol{M}}(t) - \mathsf{H}_0(\boldsymbol{M})]\mathrm{d}t\right) \\ \mathit{\Delta\Gamma} &:= \left\langle \int \mathrm{d}t \mathit{\Delta}\mathsf{H}_{\mathrm{grad}}(t) \right\rangle_0 , \end{aligned} \tag{4.16}$$

where

$$\begin{aligned} \langle \cdots \rangle_0 = \mathrm{e}^{-\mathit{\Gamma}_0} \int [\mathrm{d}\boldsymbol{M}(t)\mathrm{d}\boldsymbol{\Pi}(t)]_N \cdots \\ \times \exp([-\mathrm{i}\mathrm{Tr}\mathit{\Pi}(t)\dot{\boldsymbol{M}}(t) - \mathsf{H}_0(\boldsymbol{M})]\mathrm{d}t). \end{aligned}$$

The correction $\mathit{\Delta\Gamma}$ is computable utilizing precisely the same method as that in Sect. 3.4, except that now the field variables are time dependent[6] This time dependence renders the two-point propagator $\langle \boldsymbol{M}_{kl}(t)\boldsymbol{M}_{mn}(t')\rangle$ behavior for short time differences $|t-t'|$: $\sim \exp(-m|t-t'|)$. Fortuitously, computation of $\mathit{\Delta\Gamma}$ involves only the *coincident* two-point propagator (see (4.15) and (4.16)), and involves precisely the same group theoretic combinatorics as in (3.10). Thus, following the same large-N counting as in Sect. 3.4, we obtain

$$\begin{aligned} \mathit{\Delta\Gamma} &= \left\langle \frac{1}{\theta}\mathrm{Tr}\left(-\frac{1}{2}\left[\widehat{\boldsymbol{x}}_a, \boldsymbol{M}\right]^2\right)\right\rangle \\ &\sim \frac{N^2}{\overline{\theta}}\left(\int d\lambda\rho(\lambda)\ \lambda^2 - \left[\int \mathrm{d}\lambda\rho(\lambda)\ \lambda\right]^2\right) \\ &\sim \frac{1}{\overline{\theta}}\mathcal{O}(N^2). \end{aligned} \tag{4.18}$$

We conclude that, non-perturbatively, the size of the gradient effect is bounded from above, and is suppressed by $1/\overline{\theta}$ compared to the estimates based on Hermitian matrix quantum mechancs with the Hamiltonian H_0.

[6] In fact, if all the couplings in the Hamiltonian are *time-independent*, one can follow a method similar to the one of Sect. 3.4 by utilizing the defining relations

$$\begin{aligned} \exp(-\mathit{\Gamma}) &= \mathrm{Tr}_{\mathcal{H}_{\mathrm{Fock}}} \exp\left(-\beta\mathsf{H}\right) \\ &= \mathrm{Tr}_{\mathcal{H}_{\mathrm{Fock}}} \exp\left(-\beta\mathit{\Delta}\mathsf{H}_{\mathrm{grad}}\right) \exp\left(-\beta\mathsf{H}_0\right) \end{aligned}$$

and

$$\exp(-\mathit{\Gamma}_0) = \mathrm{Tr}_{\mathcal{H}_{\mathrm{Fock}}} \exp\left(-\beta\mathsf{H}_0\right).$$

Thus, applying the Gibbs inequality, one obtains

$$\mathit{\Gamma}_{\mathrm{exact}} \leq \mathit{\Gamma}_0 + \beta \left\langle \mathit{\Delta}\mathsf{H}_{\mathrm{grad}} \right\rangle_0 ,$$

where

$$\langle (\cdots) \rangle_0 := \frac{\mathrm{Tr}_{\mathcal{H}_{\mathrm{Fock}}}(\cdots)\exp\left(-\beta\mathsf{H}\right)}{\mathrm{Tr}_{\mathcal{H}_{\mathrm{Fock}}}\exp\left(-\beta\mathsf{H}\right)}. \tag{4.17}$$

Evaluation of (4.17) is achievable precisely as in the two-dimensional Euclidean NCFTs, as the latter can be viewed as the *classical* statistical mechanics of the $(2+1)$-dimensional NCFTs. Thus, utilizing the results of Sect. 3.4, we obtain the same results and conclusions as in (4.18)

4.6 Quantum vacua and solitons

Having identified the three possible phases at the quantum level, we now examine the vacua and solitons, and their quantum aspects. Let us introduce the second-quantized fermion field, $\mathit{\Psi}(x,t)$. The Hamiltonian is then expressible as

$$H = \int \mathrm{d}\lambda \mathit{\Psi}^\dagger(\lambda,t)\left(-\frac{1}{\theta}\frac{\partial^2}{\partial\lambda^2} + \theta V(\lambda)\right)\mathit{\Psi}(\lambda,t), \tag{4.19}$$

and we can interpret it as the Hamiltonian for a second-quantized fermion interacting with the external potential, $V(\lambda)$. In the saddle-point approximation, the equation of motion of the density field $\rho(\lambda,t)$ is given by[7]

$$\partial_t\left(\frac{1}{\rho}\partial_t\partial_\lambda^{-1}\rho\right) = \partial_\lambda\left(\frac{1}{2}\rho^2 + V(\lambda)\right). \tag{4.20}$$

Utilizing the WKB approximation for the energy levels, one finds the static solution of the density field:

$$\rho_{\mathrm{s}}(\lambda) = \begin{cases} g_{\mathrm{eff}}^{-2}\sqrt{2\left(g_{\mathrm{eff}}^2 E - V(\lambda)\right)} \\ \quad \text{for} \quad V(\lambda) \leq g_{\mathrm{eff}}^2 E, \\ 0 \quad \text{otherwise}, \end{cases} \tag{4.21}$$

where g_{eff}^2 refers to the 't Hooft coupling parameter, $g_{\mathrm{eff}}^2 = (N/\theta)$ and E refers to the first integral of (4.20), piecewise constant on each classically allowed region and fixed by the normalization condition

$$\int_{-\infty}^{+\infty} \mathrm{d}\lambda\rho_{\mathrm{s}}(\lambda) = 1. \tag{4.22}$$

Thus, in the case of a double-well potential, taking the first integrals of motion, E_1, E_2, on the left and the right wells, respectively, to be below the energy at the top of the potential, the static density field $\rho_{\mathrm{s}}(\lambda)$ is supported at the two disconnected parts (see Fig. 5) $\mathcal{D}_{\mathrm{L}}, \mathcal{D}_{\mathrm{R}}$, respectively. The normalization condition (4.22) then implies that

$$\int_{\mathcal{D}_{\mathrm{L}}} \mathrm{d}\lambda\rho_{\mathrm{s}}(\lambda) = n_1 \quad \text{and} \quad \int_{\mathcal{D}_{\mathrm{R}}} \mathrm{d}\lambda\,\rho_{\mathrm{s}}(\lambda) = n_2,$$

where $n_1 + n_2 = 1$. The two extreme limits, $n_1 = 0$ and $n_2 = 0$, correspond to the two "quantum" vacua, distributed around the respective locations of the classical vacua, while the non-zero pairs of $[n_1, n_2]$ correspond to the "quantum" solitons. Note that the first integrals of motion, E_1, E_2, take different values generically, as quantum mechanical tunnelling between the two potential wells is suppressed in the $N, \theta \to \infty$ limit.

Classical limit: $\hbar \to 0$

As a consistency check of the aforementioned three phases of the *quantum* NCFT, we will now examine the *classical*

[7] This equation of motion is approximate [32], though it is sufficient for our present purpose

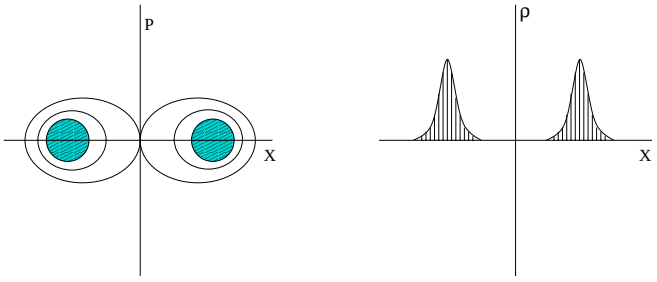

Fig. 7. Density profile of the "analog" fermions in the one-particle phase space and in the eigenvalue space. The width of the density profile is given by $\Delta\lambda \sim (\widetilde{e_{\rm F}}/\theta)^{1/2}$ and $\Delta p \sim (\widetilde{e_{\rm F}}\theta)^{1/2}$ so that $\Delta\lambda\Delta p \sim \widetilde{e_{\rm F}}$, consistent with Fermi statistics. In the classical limit, the profile reduces to delta-function distributions

limit by taking $\hbar \to 0$, while holding N large but fixed. First, from (4.11), we observe that the Planck constant $\hbar$ ought to be associated with $g^2_{\rm eff}$, as taking $g^2_{\rm eff} \equiv (N/\theta) \to 0$ along with $N \to \infty$ renders the planar phase to approach to the classical phase. In the notation of (4.11), this implies that the 't Hooft coupling scales as $g^2_{\rm eff} \sim N^{-\nu} \to 0$. Hence, in this subsection, we will take the Planck constant $\hbar$ equal to the 't Hooft coupling $g^2_{\rm eff}$.

Consider the double-well potential studied in the previous subsections. In the classical limit, we expect that the profiles of the eigenvalue density field are reduced to those of the classical phase, viz. the vacua and solitons found in [3]. This can be understood as follows. For E_1, E_2 below the potential barrier, each disconneced support of the eigenvalue density field $\rho_{\rm s}(\lambda)$ in (4.21) shrinks as $\hbar \sim g^2_{\rm eff} \to 0$, to a certain distribution of zero width, centered around $\lambda = \lambda_1$ and $\lambda = \lambda_2$, respectively. Examining the limit carefully, we find that

$$\frac{\rho_{\rm s}(\lambda)}{\hbar} \longrightarrow n_1\delta(\lambda-\lambda_1) + n_2\delta(\lambda-\lambda_2),$$

accurately reproducing the classical profile of the eigenvalue density field, (4.6). Stated differently, starting from the classical vacua and solitons (4.6) of Gopakumar, Minwalla and Strominger [3], turning on the quantum effects renders them to the filled Fermi sea of the Hermitian matrix quantum mechanics, either on a single well or multiple wells; see Fig. 7.

To convince the readers that the classical limit is correctly reproducible, consider the simplest situation again – the single-well potential $V(\lambda) = (1/2)\Omega^2\lambda^2$. Then, in the large-$N$ limit, $E = N\hbar\Omega$ (ignoring the zero-point fluctuation energy), and (4.21) implies that

$$\int_{-\infty}^{+\infty} {\rm d}\lambda\rho_{\rm s}(\lambda) = \frac{1}{N\hbar}\int_{-\lambda_0}^{+\lambda_0} {\rm d}\lambda\sqrt{2\left(N\hbar\Omega - \frac{1}{2}\Omega^2\lambda^2\right)} = 1$$

over the band $[-\lambda_0, +\lambda_0]$. Here, we have used the following value of the turning point, defining the band edge of the distribution:

$$\lambda_0 = \sqrt{2N\hbar/\Omega}.$$

One immediately notes that Planck's constant $\hbar$ is in the right place in (4.21), identifiable as $g^2_{\rm eff} \sim \hbar$. As $\hbar \to 0$, for a fixed but large N, the band edge λ_0 scales to zero, and hence the band width shrinks to zero size. At the same time, the mid-band density scales as $(\Omega/N\hbar)^{1/2} \to \infty$. Evidently, in the classical limit, the product of the mid-band density times the band width remains constant and is always of order $\mathcal{O}(1)$.

As is well exploited in the context of the matrix model description of the $c = 1$ non-critical string [18], the profile of the density field $\rho(\lambda)$ is expressible alternatively using Wigner's phase-space distribution function of the N "analog" fermions:

$$\begin{aligned} F(p,\lambda;t) &= \int {\rm d}x\Psi^\dagger\left(\lambda - \frac{\hbar}{2}x, t\right){\rm e}^{({\rm i}/\hbar)px}\Psi\left(\lambda + \frac{\hbar}{2}x, t\right) \\ &= \int {\rm d}x\Psi^\dagger\,(\lambda,t)\star{\rm e}^{({\rm i}/\hbar)px}\star\Psi\,(\lambda,t)\,. \end{aligned}$$

Here, the coordinates (λ, p) obey Moyal's commutation relation, $[p,\lambda]_\star = {\rm i}\hbar$ [8]. In terms of Wigner's distribution function, the eigenvalue density field is expressed compactly by

$$\rho(\lambda,t) = \frac{\hbar}{N}\int {\rm d}p{\rm F}(p,\lambda;t),$$

measuring the distribution of the eigenvalues. The factor of $\hbar$ reproduces correctly the normalization condition $\int {\rm d}p{\rm d}\lambda\hbar{\rm F}(p,\lambda;t) = 1$. As shown in [32], the Wigner function corresponding to a saddle-point configuration is simply given in the first-quantized description by the phase-space density of N fermions. The fermions occupy the lowest N energy eigenstates of the one-particle Hamiltonian $\mathcal{H}(\lambda)$ in (4.9).

4.7 Second-quantized description

Actually, using the second-quantized fermion field operators introduced in (4.19), the eigenvalue density field is now expressible by the fermion number density operator:

$$\hat\rho(\lambda,t) = \frac{1}{N}\Psi^\dagger(\lambda,t)\Psi\,(\lambda,t)\,, \tag{4.23}$$

yielding the correct normalization, $\int {\rm d}\lambda\Psi^\dagger(\lambda,t)\Psi(\lambda,t) = N$. Taking the expectation value of (4.23) on a many-particle state $|\lambda_1,\ldots,\lambda_N\rangle$, the antisymmetrized product of N position eigenfunctions, we obtain

$$\langle\lambda_1,\ldots,\lambda_N|\hat\rho(\lambda)|\lambda_1,\ldots,\lambda_N\rangle = \frac{1}{N}\sum_{\ell=1}^{N}\delta(\lambda-\lambda_\ell(t)), \tag{4.24}$$

[8] It is worthy noting that the matrix model for the $c = 1$ non-critical string provides an early example of a non-commutative field theory

matching perfectly with (4.5). It also satisfies the normalization condition

$$\int_{-\infty}^{+\infty} \mathrm{d}\lambda \, \langle \hat{\rho}(\lambda, t) \rangle = 1.$$

Equation (4.24) implies that the operator $\hat{\rho}(\lambda)$ is expressible by

$$\hat{\rho}(\lambda) = \frac{1}{N} \sum_{\ell=1}^{N} \delta(\hat{\lambda} - \lambda_\ell(t)), \tag{4.25}$$

where $\hat{\lambda}$ refers to the position operator in the first-quantized description. This then defines the density field operator at the quantum level.

Equipped with the eigenvalue density field operator (4.25) via the second-quantized fermion field Ψ, one can exploit the quantum effect on the NCFT vacua and solitons. Restricting low-energy excitations to the $U(\infty)$ invariant sector, we have found that the classical dynamics of the tachyon field is described by the density field $\rho(\lambda)$. Likewise, in the same $U(\infty)$ invariant sector, the quantum dynamics of the tachyon field is described by the density field operator $\hat{\rho}(\lambda)$ defined in (4.25). The extent of quantum effects can be judged by taking the expectation value of (4.25) and measuring the deviation from its classical value (4.5). For instance, by approximating the eigenvalue density field operator to be the same as the classical distribution, we have obtained in the previous subsection that

$$\langle \hat{\rho}(\lambda) \rangle = \frac{1}{\hbar} \sqrt{2(E - V(\lambda))}.$$

Equivalently, the $U(\infty)$ invariant information of the tachyon field is governed by the change of variable:

$$\frac{1}{N} \mathrm{Tr}_{\mathcal{H}} \boldsymbol{T}^n = \int_{-\infty}^{+\infty} \mathrm{d}\lambda \lambda^n \rho(\lambda).$$

Thus, from a knowledge of the classical $\rho(\lambda)$, one can reconstruct the classical tachyon field $\boldsymbol{T}$ in the Weyl formulation. One can subsequently rebuild the tachyon field $\mathrm{T}(x)$ on $\mathbb{R}^2$ via the Weyl–Moyal correspondence map. The reconstruction is equally applicable at the quantum level. For instance,

$$\frac{1}{N} \mathrm{Tr}_{\mathcal{H}} \left\langle \widehat{\boldsymbol{T}}^n \right\rangle = \int_{-\infty}^{+\infty} \mathrm{d}\lambda \lambda^n \, \langle \widehat{\rho}(\lambda) \rangle \, .$$

Denote the image of the Weyl–Moyal map of $\left\langle \widehat{\boldsymbol{T}} \right\rangle$ $\widehat{\mathrm{T}}(\boldsymbol{x})$. Then, the above equation becomes

$$\frac{1}{V(\mathbb{R}^2_\theta)} \int_{\mathbb{R}^2_\theta} \mathrm{d}^2\boldsymbol{x} \left[\widehat{\mathrm{T}}(\boldsymbol{x}) \star \widehat{\mathrm{T}}(\boldsymbol{x}) \star \cdots \star \widehat{\mathrm{T}}(\boldsymbol{x}) \right]_{n-\text{tuple}} = \int_{-\infty}^{+\infty} \mathrm{d}\lambda \lambda^n \, \langle \widehat{\rho}(\lambda) \rangle \, . \tag{4.26}$$

This moment relation enables one to reconstruct the "quantum" profile of the vacua and solitons over $\mathbb{R}^2_\theta$. We will utilize this map by illustrating two representative physical consequences driven by the "quantum effects".

Quantum destruction of long-range order

We have already demonstrated that the quantum effect drives the classical density profile of delta-function type into a Fermi distribution, as depicted in Fig. 7. A consequence of broadening into the Fermi distribution is that the translational invariance over $\mathbb{R}^2_\theta$, viz. $\boldsymbol{x}^a \to \boldsymbol{x}^a +$ (constant), which is respected by all classical vacua, is dynamically broken.

Recall that the classical vacua correspond to density distributions of delta-function type, all eigenvalues taking the same value, say, T_0. Thus, (4.26) yields

$$\frac{1}{V(\mathbb{R}^2_\theta)} \int_{\mathbb{R}^2_\theta} \mathrm{d}^2\boldsymbol{x} (\widehat{\mathrm{T}}(\boldsymbol{x}))^n_\star = \mathrm{T}_0^n \quad \text{for} \quad n = 1, 2, 3, \cdots$$

and hence we find the unique solution as $\widehat{\mathrm{T}}(\boldsymbol{x}) = \mathrm{T}_0$ – a *homogeneous* configuration, respecting the translational invariance over $\mathbb{R}^2_\theta$.

Once quantum effects are taken into account, as shown above, the classical delta-function type density distribution is broadened into a Fermi distribution putting each eigenvalue at a different value – a consequence of the repulsion between adjacent eigenvalues. In this case, it is fairly straightforward to convince oneself that there is *no* homogeneous solution solving the moment map (4.26) for *all* n. As such, a generic solution of (4.26) ought to be a non-trivial function over $\mathbb{R}^2_\theta$. To illustrate this, let us take

$$\langle \widehat{\rho}(\lambda) \rangle = \begin{cases} 1/R & \text{for} \quad -R/2 \le \lambda \le +R/2, \\ 0 & \text{otherwise.} \end{cases}$$

Then a solution of (4.26) is easily found:

$$\widehat{\mathrm{T}}(\boldsymbol{x}) = \begin{cases} x^1 & \text{for} \quad -R/2 \le x^1 \le +R/2, \\ 0 & \text{otherwise,} \end{cases} \tag{4.27}$$

thus breaking translational invariance along the x^1-direction over $\mathbb{R}^2_\theta$, though invariant under translation along the x^2-direction. There are also infinitely many other solutions of (4.26), including the "stripe-phase" states, but these are all related to the solution (4.27) via $U(\infty)$ rotations, viz. solutions of the type $U(\boldsymbol{x}) \star \mathrm{T}(x^1) \star U^{-1}(\boldsymbol{x})$ for an arbitrary $U(\boldsymbol{x})$.

We conclude that the translational long-range order of the classical vacua in NCFT is destroyed generically by quantum fluctuations.

Quantum corrected soliton mass

Consider the classical soliton of type (N_a, N_b), (4.4). We are interested in estimating the mass of the "quantum"

soliton, or, equivalently, the quantum correction to the soliton mass. Take, for definiteness, the potential $V(\boldsymbol{T})$ of the type given in Fig. 3. Classically, the soliton mass is simply given by the increase of the potential energy by moving, out of in total $N = N_{\rm L} + N_{\rm L}$ eigenvalues situated at the global vacuum on the left well, a fraction of $N_{\rm R}$ eigenvalues to the local minima on the right well. Denoting the energy difference between the left and the right wells, $V_{\rm L}, V_{\rm R}$, as $\Delta V = (V_{\rm R} - V_{\rm L})$, the classical soliton mass is given by

$$M_{(N_{\rm L},N_{\rm R})}[\text{classical}] \sim \theta N_{\rm R} \Delta V.$$

Quantum mechanically, the eigenvalue distribution for both the global vacuum and the $(N_{\rm L}, N_{\rm R})$ soliton will be broadened into Fermi distributions. Thus, the quantum corrected soliton mass is estimated by computing the difference of the energy functional averaged over the Fermi distributions according to (4.26). Utilizing the results of (4.12) and (4.13), we estimate the quantum corrected soliton mass to be

$$\begin{aligned} &M_{(N_{\rm L},N_{\rm R})}[\text{quantum}] = \left\langle \mathcal{E}_{(N_{\rm L},N_{\rm R})} \right\rangle - \left\langle \mathcal{E}_{(N_{\rm L}+N_{\rm R},0)} \right\rangle \\ &\sim \left(\theta N_{\rm L} V_{\rm L} + N_{\rm L}^2\right) + \left(\theta N_{\rm R} V_{\rm R} + N_{\rm R}^2\right) - \left(\theta N V_{\rm L} + N^2\right) \\ &= M[\text{classical}] - 2N_{\rm L} N_{\rm R}. \end{aligned}$$

We thus deduce that the quantum correction, as given by the second term in the last expression, is *negative* and is of order $\mathcal{O}(N^2)$. Evidently, the correction is negligible in the GMS-phase, comparable in the planar phase, but outweighs the classical mass in the disordered phase.

5 Discussions

Before closing, we would like to bring up the investigation of related phenomena in other contexts. The first concerns quantum effects either in IKKT Type IIB or in BFSS Type IIA matrix theories. For the Type IIB IKKT matrix model, the issue of the measure-induced interaction between eigenvalues and its consequences has been considered previously, albeit in a different context and with a different motivation. See, for instance, the results of [33] and references therein. The classical moduli space is given by ten commuting matrices whose eigenvalues span $\mathbb{R}^{10}$, ten-dimensional Euclidean spacetime. A calculation of the matrix partition function indicates that the moduli space is partly lifted and, normally speaking, a smaller-dimensional submanifold remains non-compact and flat. The result is attributed to a logarithmic interaction between the eigenvalues as the remaining "angular" degrees of freedom are integrated out. This is similar to the Vandermonde effect of the one-matrix model.

Classical solutions of the IKKT and BFSS matrix models include all of the D-branes in Type IIA and IIB strings. The low-energy theory is equivalent to NCFTs involving both scalar and gauge fields. An immediate question is whether there exist various kinds of large-N limits in these field theories, some of which might destabilize the D-branes by quantum fluctuations. We believe that this is a very important issue, so let us look a little closer. One place to look for this sort of effect would be one-loop computations in the IKKT and BFSS matrix models which might show the necessity of a sort of 't Hooft-like scaling, viz. $\theta \sim N$, without which the D-brane solutions might be completely destabilized, which is the counterpart of the disordered phase studied in this paper. Of course, for Dp-branes or a system of Dp–Dq-branes (with $p = q \mathrm{mod} 4$) bosonic and fermionic determinants cancel because of supersymmetry and there are no large-N divergences at one loop. On the other hand, supersymmetry is broken in situations involving

(i) relative motion between the BPS-branes,
(ii) Dp–Dq-branes with $p - q$ not a multiple of 4, and
(iii) brane–antibrane systems.

In (iii), the $D2$–$\bar{D}2$ system [34,35] was studied extensively, and it would be an interesting starting place to address the large-N issues raised here.

Second, as elaborated in Sect. 2.7, the measure effect we have discussed in this paper is intimately related to the phenomenon of IR divergence [21] through non-planar diagrams. Recently, it has been shown [36] that the completion of all the non-planar diagrams participating in the UV–IR mixing in NCFTs studied in this work is expressible entirely in terms of the scalar counterpart of the open Wilson lines [37]. The effective action is then interpreted as (the Legendre transform of) an effective field theory of non-commutative dipoles – the non-commutative manifestation of dynamically generated "closed strings" [38]. There, the result was based exclusively on the Moyal formulation. An interesting problem is to recast this result in the Weyl formulation, and to understand the three different scaling regimes in terms of the open Wilson lines and non-commutative dipoles.

Finally, it would be interesting to see if the transition to the disordered phase discussed in this paper is related to the large-N phase transition [26].

We will report progress regarding the above problems elsewhere.

Acknowledgements. We are grateful to S.R. Das, A. Dhar, M.R. Doulgas, R. Gopakumar, D.J. Gross, V. Kazakov, S. Minwalla, S. Mukhi, A. Sen, and S.H. Shenker for enlightening discussions. We would like to thank hospitality of the Theory Division at CERN (GM and SJR), Institut Henri Poincaré (SJR), and Institut des Hautes Études Scientifiques (SJR) during this work.

Appendix

A Weyl–Moyal correspondence

In this section we briefly review the operator formulation of NCFT in the context of Sect. 2.1.

One begins by introducing an "auxiliary" one-particle Hilbert space $\mathcal{H}$, of dimension $\dim\mathcal{H} = N$ [9], carrying a

[9] Since representations of (A.1) are necessarily infinite-dimensional, $N = \infty$ at the moment. We will shortly discuss

representation of the Heisenberg algebra:

$$\left[\widehat{x^a}, \widehat{x^b}\right] = \mathrm{i}\epsilon^{ab}\mathrm{I\!I}.$$

The Weyl–Moyal map refers to the isomorphism between functions on $\mathbb{R}^2_\theta$ and operators on $\mathcal{H}$:

$$\begin{aligned} \boldsymbol{x} &\longleftrightarrow \widehat{\boldsymbol{x}}, \\ \mathrm{T}(\boldsymbol{x}) &\longleftrightarrow \boldsymbol{T}(\widehat{\boldsymbol{x}}), \\ V_\star(T) &\longleftrightarrow V(\boldsymbol{T}), \\ \int \mathrm{d}^2\boldsymbol{x}\cdots &\longleftrightarrow \mathrm{Tr}_{\mathcal{H}_\theta}\cdots \end{aligned} \tag{A.1}$$

In particular, in a plane-wave basis, the Weyl–Moyal map renders the following one-to-one correspondence between the fields:

$$\mathrm{T}(\boldsymbol{x}) = \int_{\widetilde{\mathbb{R}^2}} \frac{\mathrm{d}^2\boldsymbol{k}}{(2\pi)^2} \mathrm{e}^{-\mathrm{i}\boldsymbol{k}\cdot\boldsymbol{x}} \mathrm{Tr}_{\mathcal{H}}\left(\mathrm{e}^{\mathrm{i}\boldsymbol{k}\cdot\widehat{\boldsymbol{x}}}\boldsymbol{T}\right), \tag{A.2}$$

which follows from the Weyl ordering prescription of the operators $\widehat{\boldsymbol{x}}$.

The map, (A.1), then equates the NCFT action (2.4) with (2.6). Operators on $\mathcal{H}$ are realizable in terms of matrices once we introduce a complete set of orthonormal basis elements of $\mathcal{H}$ as $|\ell\rangle$, $\ell = 1, 2, \cdots, \dim\mathcal{H} \equiv N$, and one-dimensional projection operators therein:

$$\boldsymbol{P}_\ell = |\ell\rangle\langle\ell| \qquad \ell = 1, 2, \cdots, \dim\mathcal{H} \equiv N. \tag{A.3}$$

The $\boldsymbol{P}_\ell$'s satisfy the projective and the completeness relations:

$$\boldsymbol{P}_\ell\boldsymbol{P}_m = \delta_{\ell m}\boldsymbol{P}_m \quad \text{and} \quad \sum_{\ell=1}^{N} \boldsymbol{P}_\ell = \mathrm{I\!I}.$$

At leading order in $(1/\theta)$, both (2.4) and (2.6) are invariant under

$$\mathrm{T}(\boldsymbol{x}) \to U(\boldsymbol{x}) \star \mathrm{T}(\boldsymbol{x}) \star U^{-1}(\boldsymbol{x}) \longleftrightarrow \boldsymbol{T} \to \boldsymbol{U}\boldsymbol{T}\boldsymbol{U}^{-1}, \tag{A.4}$$

representing an area-preserving diffeomorphism; equivalently, $U(\infty)$ symmetry. The symmetry is broken explicitly by the term $\mathcal{L}_{-1}$.

B Large-N saddle point of one-matrix model

As mentioned in Sect. 2.4, taking $\theta = N/g^2_{\mathrm{eff}}$ and small enough g_{eff}, we have seen that the large-N saddle point for the density ρ_{s} (ρ defined in (2.7)) is simply an extremum of the effective action (2.23) (with the constraint (2.22) taken care of by a Lagrange multiplier E):

$$S_{\mathrm{total}}[\rho] = S_{\mathrm{eff}}[\rho] + E\left(1 - \int_{\mathcal{D}} \mathrm{d}\lambda\rho(\lambda)\right). \tag{B.1}$$

The saddle-point equation for ρ then reads

$$\begin{aligned} \partial_\rho S_{\mathrm{total}}[\rho] = N^2 \left[g^{-2}_{\mathrm{eff}} V(\lambda) - 2\int_{\mathcal{D}} \mathrm{d}\mu\rho(\mu)\ln|\lambda-\mu|\right] \\ - N\theta E = 0 \quad \text{for} \quad \lambda \subset \mathcal{D}, \end{aligned} \tag{B.2}$$

viz. analytically continuing to the complex λ plane, the real part of

$$V_{\mathrm{eff}}(\lambda) = V(\lambda) - 2g^2_{\mathrm{eff}}\int_{\mathcal{D}} \mathrm{d}\mu\rho(\mu)\ln(\lambda-\mu)$$

remains constant, E, over the support $\mathcal{D}$. Taking the derivative of (B.2) with respect to λ, one obtains the following dispersion relation:

$$\frac{1}{2g^2_{\mathrm{eff}}} V'(\lambda) = \fint_{\mathcal{D}} \mathrm{d}\mu \frac{\rho(\mu)}{\lambda-\mu} \quad \text{for} \quad \lambda \subset \mathcal{D}.$$

The right-hand side is related to the resolvent $\mathcal{R}(\lambda)$ of the eigenvalue distribution:

$$\begin{aligned} \mathcal{R}(\lambda) &:= \lim_{N\to\infty} \left\langle \frac{1}{N}\mathrm{Tr}\frac{1}{\lambda - \boldsymbol{T}} \right\rangle = \int_{\mathcal{D}} \mathrm{d}\mu \frac{\rho(\mu)}{(\lambda-\mu)}, \\ \mathrm{Re}\mathcal{R}(\lambda) &= \fint_{\mathcal{D}} \mathrm{d}\mu \frac{\rho(\mu)}{(\lambda-\mu)}, \end{aligned} \tag{B.3}$$

supplemented with the boundary condition

$$\mathcal{R}(\lambda) = \frac{1}{\lambda} + \mathcal{O}\left(\frac{1}{\lambda^2}\right) \quad \text{for} \quad \lambda \to \infty$$

as a consequence of the normalization condition

$$\int \mathrm{d}\lambda\rho(\lambda) = 1.$$

Consider now the potential (2.8). Let us look for a saddle point corresponding to the (N_1, N_2) instantons. Evidently, extending the above results, the quantum counterpart of (N_1, N_2) instantons ought to correspond to so-called two-cut distributions in the matrix model. The two-cut distribution is characterized by two disjoint intervals $\mathcal{D}_1, \mathcal{D}_2$ and fractions of the eigenvalue density:

$$n_1 = \int_{\mathcal{D}_1} \mathrm{d}\lambda\rho(\lambda) \quad \text{and} \quad n_2 = \int_{\mathcal{D}_2} \mathrm{d}\lambda\rho(\lambda)$$

with $n_1 + n_2 = 1$. In the large-N, large-θ limit, the total action is now given by

$$\begin{aligned} S_{\mathrm{total}}[\rho; n_1, n_2] = S_{\mathrm{eff}}[\rho] + E_1\left(n_1 - \int_{\mathcal{D}_1} \mathrm{d}\lambda\rho(\lambda)\right) \\ + E_2\left(n_2 - \int_{\mathcal{D}_2} \mathrm{d}\lambda\rho(\lambda)\right). \end{aligned}$$

The saddle-point equation for $\rho(\lambda)$ takes the same form as before, viz.:

$$\begin{aligned} N^2\left(g^{-2}_{\mathrm{eff}} V(\lambda) - 2\int_{\mathcal{D}_1} \mathrm{d}\mu\rho(\mu)\ln|\lambda-\mu|\right) = N\theta E_1 \\ \text{for} \quad \lambda \subset \mathcal{D}_1, \\ N^2\left(g^{-2}_{\mathrm{eff}} V(\lambda) - 2\int_{\mathcal{D}_2} \mathrm{d}\mu\rho(\mu)\ln|\lambda-\mu|\right) = N\theta E_2 \\ \text{for} \quad \lambda \subset \mathcal{D}_2. \end{aligned}$$

(Sect. 2.3) how on a non-commutative torus with rational θ, N becomes finite

The saddle-point equation with respect to n_1 yields

$$\partial_{n_1} S_{\text{total}}[\rho; n_1, n_2] = (E_1 - E_2) = 0. \qquad \text{(B.4)}$$

For the double-well potential of the type (2.8), the distribution on the two wells is symmetric. Using the methods mentioned above (see [15,24] for more details), one finds that the saddle point is given in terms of a two-cut eigenvalue distribution (2.27).

References

1. A. Connes, M.R. Douglas, A. Schwarz, JHEP **9802**, 003 (1998) [hep-th/9711162]
2. N. Seiberg, E. Witten, JHEP **9909**, 032 (1999) [hep-th/9908142]
3. R. Gopakumar, S. Minwalla, A. Strominger, JHEP **0005**, 020 (2000) [hep-th/0003160]
4. M. Aganagic, R. Gopakumar, S. Minwalla, A. Strominger, JHEP **0104**, 001 (2001) [hep-th/0009142]
5. L. Hadasz, U. Lindstrom, M. Rocek, R. von Unge, JHEP **0106**, 040 (2001) [hep-th/0104017]
6. R. Gopakumar, M. Headrick, M. Spradlin, hep-th/0103256
7. N. Nekrasov, A. Schwarz, Commun. Math. Phys. **198**, 689 (1998) [hep-th/9802068]
8. D.J. Gross, N.A. Nekrasov, JHEP **0007**, 034 (2000) [hep-th/0005204]
9. A.P. Polychronakos, Phys. Lett. B **495**, 407 (2000) [hep-th/0007043]
10. D.P. Jatkar, G. Mandal, S.R. Wadia, JHEP **0009**, 018 (2000) [hep-th/0007078]
11. K. Dasgupta, S. Mukhi, G. Rajesh, JHEP **0006**, 022 (2000) [hep-th/0005006]
12. E. Witten, hep-th/0006071
13. J.A. Harvey, P. Kraus, F. Larsen, E.J. Martinec, JHEP **0007**, 042 (2000) [hep-th/0005031]
14. G. Mandal, S.-J. Rey, Phys. Lett. B **495**, 193 (2000) [hep-th/0008214]
15. E. Brezin, C. Itzykson, G. Parisi, J.B. Zuber, Commun. Math. Phys. **59**, 35 (1978)
16. E. Brezin, S.R. Wadia, The Large N expansion in quantum field theory and statistical physics: From spin systems to two-dimensional gravity (World Scientific, Singapore 1993); M.L. Mehta, Random matrices, 2nd ed. (Academic Press, New York, 1991); P.A. Mello, Theory of random matrices, Les Houches Session LXI, edited by E. Akkermans, G. Montambaux, J.L. Pichard, J. Zinn-Justin (North-Holland Pub. Co., Amsterdam 1994)
17. M.R. Douglas, S.H. Shenker, Nucl. Phys. B **335**, 635 (1990); D.J. Gross, A.A. Migdal, Phys. Rev. Lett. **64**, 127 (1990); Phys. Rev. Lett. **64**, 717 (1990); M.R. Douglas, Phys. Lett. B **238**, 176 (1990)
18. D.J. Gross, N. Miljkovic, Phys. Lett. B **238**, 217 (1990); E. Brezin, V.A. Kazakov, A.B. Zamolodchikov, Nucl. Phys. B **338**, 673 (1990); P. Ginsparg, J. Zinn-Justin, Phys. Lett. B **240**, 333 (1990); G. Parisi, Phys. Lett. B **238**, 209 (1990)
19. N. Ishibashi, H. Kawai, Y. Kitazawa, A. Tsuchiya, Nucl. Phys. B **498**, 467 (1997) [hep-th/9612115]
20. T. Banks, W. Fischler, S.H. Shenker, L. Susskind, Phys. Rev. D **55**, 5112 (1997) [hep-th/9610043]
21. S. Minwalla, M. Van Raamsdonk, N. Seiberg, JHEP **0002**, 020 (2000) [hep-th/9912072]
22. S.-J. Rey, talk given at Strings 2001, International Conference at Tata Institute for Fundamental Research (Mumbai, India) http://theory.theory.tifr.res.in/strings/Proceedings/#rey-t
23. A. Sen, JHEP **9808**, 012 (1998) [hep-th/9805170]; JHEP **9912**, 027 (1999) [hep-th/9911116]; A. Sen, B. Zwiebach, JHEP **0003**, 002 (2000) [hep-th/9912249]
24. G. Bhanot, G. Mandal, O. Narayan, Phys. Lett. B **251**, 388 (1990)
25. M. Van Raamsdonk, hep-th/0110093
26. D.J. Gross, E. Witten, Phys. Rev. D **21**, 446 (1980); S. Wadia, EFI-79/44-Chicago preprint (KEK Scanned Version); Phys. Lett. B **93**, 403 (1980)
27. R.P. Feynman, Statistical mechanics (Benjamin Pub. Co., Boston 1972)
28. B. Sakita, Quantum theory of many-variable systems and fields (World Scientific Pub. Co., Singapore 1985)
29. M. Creutz, Rev. Mod. Phys. **50**, 561 (1978)
30. A. Jevicki, B. Sakita, Nucl. Phys. B **165**, 511 (1980); S.R. Das, A. Jevicki, Mod. Phys. Lett. A **5**, 1639 (1990); A.M. Sengupta, S.R. Wadia, Int. J. Mod. Phys. A **6**, 1961 (1991); D.J. Gross, I.R. Klebanov, Nucl. Phys. B **352**, 671 (1991)
31. D.J. Gross, I. Klebanov, Nucl. Phys. B **344**, 475 (1990)
32. A. Dhar, G. Mandal, S.R. Wadia, Mod. Phys. Lett. A **7**, 3129 (1992) [hep-th/9207011]; Mod. Phys. Lett. A **8**, 3557 (1993) [hep-th/9309028]
33. J. Ambjorn, K.N. Anagnostopoulos, W. Bietenholz, F. Hofheinz, J. Nishimura, hep-th/0104260
34. O. Aharony, M. Berkooz, Nucl. Phys. B **491**, 184 (1997) [hep-th/9611215]; G. Lifschytz, S. Mathur, Nucl. Phys. B **507**, 621 (1997) [hep-th/9612087]
35. G. Mandal, S.R. Wadia, Nucl. Phys. B **599**, 137 (2001) [hep-th/0011094]; P. Kraus, A. Rajaraman, S.H. Shenker, Nucl. Phys. B **598**, 169 (2001) [hep-th/0010016]
36. Y. Kiem, S.-J. Rey, H.-T. Sato, J.-T. Yee, hep-th/0106121; hep-th/0107106; Y. Kiem, S.-S. Kim, S.-J. Rey, H.-T. Sato, hep-th/0110066; Y. Kiem, S. Lee, S.-J. Rey, H.-T. Sato, hep-th/0110215
37. N. Ishibashi, S. Iso, H. Kawai, Y. Kitazawa, Nucl. Phys. B **573**, 573 (2000) [hep-th/9910004]; S.-J. Rey, R. von Unge, Phys. Lett. B **499**, 215 (2001) [hep-th/0007089]; S.R. Das, S.-J. Rey, Nucl. Phys. B **590**, 453 (2000) [hep-th/0008042]; D.J. Gross, A. Hashimoto, N. Itzhaki, hep-th/0008075; A. Dhar, S.R. Wadia, Phys. Lett. B **495**, 413 (2000) [hep-th/0008144]
38. S.-J. Rey, Exact Answers to Approximate Questions: Noncommutative Dipole, Open Wilson Line, and UV–IR Duality, Proceedings of New Ideas in String Theory, APCTP-KIAS Workshop (June, 2001) and of Gravity, Gauge Theories, and Strings, Les Houches Summer School (August, 2001), to appear